

**NACA**

Declassified by authority of NASA  
Classification Change Notices No. 167  
Date \*\* JAN 15 1969

# RESEARCH MEMORANDUM

COMPARISON OF WIND-TUNNEL, ROCKET, AND FLIGHT DRAG  
MEASUREMENTS FOR EIGHT AIRPLANE CONFIGURATIONS  
AT MACH NUMBERS BETWEEN 0.7 AND 1.6

By Paul E. Purser

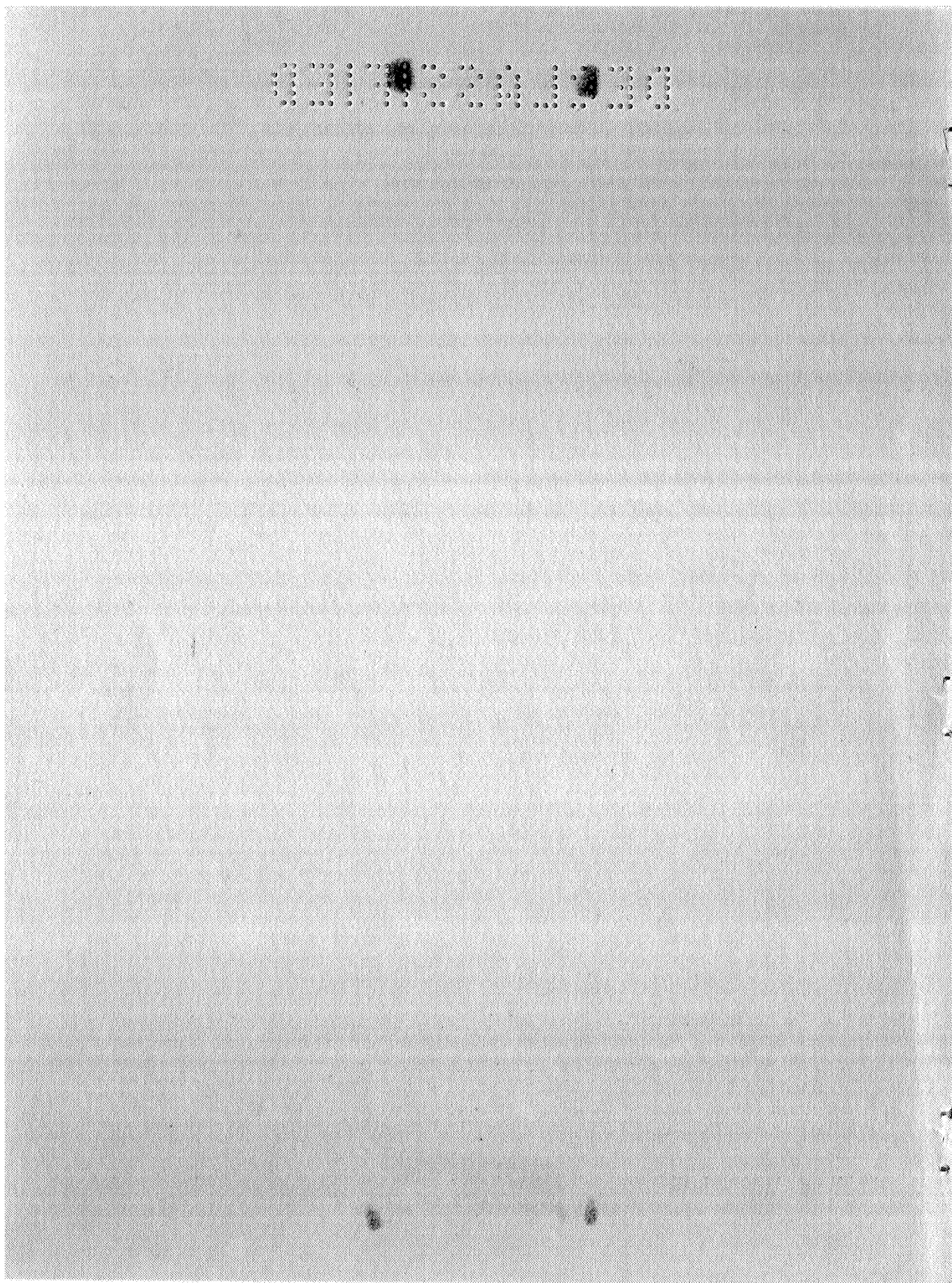
Langley Aeronautical Laboratory  
Langley Field, Va.

This material is to be controlled in the same manner as the material of which it is a part.

**NATIONAL ADVISORY COMMITTEE  
FOR AERONAUTICS**

WASHINGTON

September 16, 1954



## NATIONAL ADVISORY COMMITTEE FOR AERONAUTICS

## RESEARCH MEMORANDUM

COMPARISON OF WIND-TUNNEL, ROCKET, AND FLIGHT DRAG  
MEASUREMENTS FOR EIGHT AIRPLANE CONFIGURATIONS  
AT MACH NUMBERS BETWEEN 0.7 AND 1.6

By Paul E. Purser

## SUMMARY


Comparisons have been made of low-lift drag measurements obtained on eight airplane configurations at Mach numbers between 0.7 and 1.6 by various techniques. Data were obtained from wind-tunnel tests and from rocket-propelled model and airplane flight tests.

In general, the agreement of data from various sources is good and no consistent effects of Reynolds number were discernible in the data. Most of the apparent discrepancies and the lack of Reynolds number effects are at least qualitatively explainable by consideration of such factors as surface condition, individual test setup and accuracy, and detail geometric differences between the airplanes and their respective models.

## INTRODUCTION

The National Advisory Committee for Aeronautics, at the request of the U. S. Air Force and Bureau of Aeronautics, Department of the Navy, conducts many investigations of specific existing or proposed service aircraft. In the course of these investigations, questions continually arise as to the dependence one can place on drag measurements obtained by various research techniques, particularly at transonic and low supersonic speeds, and on the reliability of drag reductions obtained by extrapolating the data to higher Reynolds numbers.

In order to answer at least partially the questions of validity of model drag data, a collection and comparison has been made of such data for eight airplane configurations. The basic data considered appear in references 1 to 19 and in various unpublished forms. The data were obtained from tests in NACA and company-owned wind tunnels, from NACA rocket-propelled-model flight tests, and from NACA, U. S. Air Force, and



company-conducted airplane flight tests. The airplanes considered are the Bell X-1, Douglas X-3, Douglas D-558-II, Bell X-5, McDonnell XF3H-1, Douglas XF4D-1, North American YF-100A, and Republic XF-91 airplanes.

The general sources of data for each configuration are:

<u>Airplane</u>	<u>Source</u>
Bell X-1 . . . . .	tunnel and flight
Douglas X-3 . . . . .	tunnel, rocket, and flight
Douglas D-558-II . . . . .	tunnel, rocket, and flight
Bell X-5 . . . . .	tunnel and flight
McDonnell XF3H-1 . . . . .	tunnel, rocket, and flight
Douglas XF4D-1 . . . . .	tunnel, rocket, and flight
North American YF-100A . . . . .	tunnel and rocket
Republic XF-91 . . . . .	rocket and flight

This report presents, compares, and briefly discusses the available low-lift transonic drag data for these eight airplane configurations.

#### SYMBOLS


$C_D$	drag coefficient, $D/qS$
$C_L$	lift coefficient, $L/qS$
$C_f$	friction-drag coefficient, $\frac{\text{Friction drag}}{q \times \text{Wetted area}}$
$S$	total wing area, sq ft
$D$	drag, lb
$L$	lift, lb
$q$	dynamic pressure, $\frac{\gamma}{2} \rho M^2$ , lb/sq ft
$M$	Mach number
$p$	static pressure, lb/sq ft
$\gamma$	specific heat ratio for air, 1.4
$R$	Reynolds number, $\rho V \bar{c} / \mu$
$\rho$	mass density of air, slug/cu ft

$\mu$	viscosity of air, slugs/ft-sec
$V$	velocity, ft/sec
$\bar{c}$	wing mean aerodynamic chord, ft
$m/m_0$	inlet mass-flow ratio, ratio of mass rate of flow into inlet to mass rate of flow through free-stream tube of area equal to inlet area

## ABBREVIATIONS

The following abbreviations are used to designate the various research facilities:

NACA flight	airplane flight tests conducted by NACA at High-Speed Flight Research Station at Edwards Air Force Base, Calif.
DAC flight	airplane flight tests conducted by Douglas Aircraft Company
MAC flight	airplane flight tests conducted by McDonnell Aircraft Company
RAC flight	airplane flight tests conducted by Republic Aviation Corporation
USAF flight	airplane flight tests conducted by United States Air Force
Rocket	rocket-model flight tests conducted by the Langley Pilotless Aircraft Research Division (PARD) at its testing station at Wallops Island, Va.
8' HST	Langley 8-foot high-speed tunnel
8' TT	Langley 8-foot transonic tunnel
16' TT	Langley 16-foot transonic tunnel
6' SST	Ames 6- by 6-foot supersonic tunnel
4' SPT	Langley 4- by 4-foot supersonic pressure tunnel
OAL	Ordnance Aerophysics Laboratory Tunnel, Daingerfield, Texas



CWT Bump	bump tests in Southern California Cooperative Wind Tunnel
CWT	Southern California Cooperative Wind Tunnel
16" ST	North American Aviation, Inc., 16 x 16-inch Supersonic Wind Tunnel

## DATA

### Source and Presentation

Drag data for the various airplane configurations were obtained from the sources listed in table I (refs. 1 to 19) and from some unpublished sources such as data letters from the manufacturers, and from the files of the Langley Aeronautical Laboratory.

Geometric data for the various configurations are presented in table I and both geometric and aerodynamic data are presented in figures 1 to 8.

### Treatment of Base, Duct, and Inlet Drag

Base drag.- Whatever base drag existed is included in all airplane flight data. Base drag, calculated from measured base pressures, has been subtracted from all wind-tunnel data except for the Bell X-1 (8' HST and 16' TT) and Douglas D-558-II (8' HST, model A) and from all rocket-model data except for the Republic XF-91. The tare procedure of the Langley 8-foot high-speed tunnel eliminated the necessity for subtracting base pressure for the X-1 and D-558-II data of references 2 and 6, and measured base pressures on the Bell X-1 model in the 16-foot transonic tunnel (unpublished) agreed with flight base-pressure measurements. For the XF-91 rocket model (ref. 18), no base-pressure measurements were made.

Internal duct drag.- Measured values of internal duct drag have been subtracted from all data obtained on ducted models in wind tunnels and on ducted rocket models. Internal duct drags have effectively been subtracted from the airplane flight data by the definition of thrust as the change in momentum between the inlet and the exit.

Inlet drag.- The following notes outline the treatment of inlet drag for the various configurations:

CONFIDENTIAL

Configuration

No inlet . . . . . Bell X-1  
 Airplane and rocket and tunnel models operated at  
 approximately same  $m/m_0$  . . . . . Douglas X-3  
 No inlet . . . . . Douglas D-558-II  
 Tunnel and flight tests were made with approximately  
 same  $m/m_0$  . . . . . Bell X-5  
 Rocket, tunnel, and flight tests were all made with  
 approximately same  $m/m_0$  . . . . . Douglas XF4D-1  
 Tunnel tests were made with plugged and faired-  
 over inlets which were assumed equivalent to  
 $m/m_0 = 1$ . Rocket-model data (unpublished)  
 were corrected from  $m/m_0 = 0$  (blocked ducts)  
 to  $m/m_0 = 1$  by data from inlet model  
 (ref. 11). Airplane data were corrected  
 from  $0.7 < m/m_0 < 1.0$  to  $m/m_0 = 1$  by data  
 from flight (ref. 10) . . . . . McDonnell XF3H-1  
 Rocket model with faired nose was assumed equivalent to  
 $m/m_0 = 0.9^+$ . Airplane data were obtained at  
 $m/m_0 = 0.9^+$ . . . . . Republic XF-91

## Area Distributions

Longitudinal distributions of cross-sectional area and the equivalent bodies of revolution for several of the configurations are presented in figures 2 to 7 as a matter of general interest. The actual equivalence of pressure drag for complete configurations and equivalent bodies is discussed more fully in references 20 and 21.

## Reynolds Numbers

The values of Reynolds number shown with the airplane flight data in figures 1 to 8 generally were those listed as extremes in the reference material. The straight-line fairing of  $R$  against  $M$  is intended only to show the Reynolds number range and not to indicate an actual variation of  $R$  with  $M$ .

## DISCUSSION

## Bell X-1 Airplane

Drag data for  $C_L = 0.2$  are presented in figure 1 for the Bell X-1 research airplane with 10-percent-thick wing. Data were taken from NACA

flight tests (ref. 1) and from tests in the Langley 8-foot high-speed and 16-foot transonic tunnels (ref. 2 and unpublished data). The flight-test drag points were obtained from cross plots of  $C_D$  against  $\alpha$  made from data obtained from level flight, push-downs, and pull-ups with power off. The stabilizer and elevator settings are not given in reference 1. The tunnel data are for stabilizer and elevator settings of zero.

The agreement of the data from the three sources is considered excellent. The maximum scatter about a mean subsonic level is  $\pm 0.002$  or about  $\pm 12$  percent in drag coefficient and the maximum scatter in the steep portion of the drag rise is about  $\pm 0.01$  in Mach number.


#### Douglas X-3 Airplane

Drag data at  $C_L = 0$  and  $0.3$  are presented in figure 2 for the Douglas X-3 research airplane. Data were taken from preliminary unpublished flight tests made by Douglas with NACA instrumentation, rocket-propelled-model tests by Langley PARD (ref. 3), and tests in the Ames 6- by 6-foot supersonic tunnel (ref. 4). Both rocket and wind-tunnel models were tested with two sizes of horizontal tail; the airplane was flown only with the larger tail. Rocket-model data are for tail settings between  $0$  and  $-3^\circ$  and the wind-tunnel data are for a tail setting of zero. Airplane tail settings varied  $-2.8^\circ$  and  $-4.8^\circ$ .

The maximum disagreements in zero-lift drag coefficient level between the rocket and tunnel models are about  $0.006$  which corresponds to about 20 to 25 percent at subsonic speeds and to about 10 percent at supersonic speeds. The difference in direction of this disagreement on either side of  $M = 1$  may be due to the fact that the tunnel tests had to be made with a large sting which extended under the tail boom of the model in order to support the model at the fuselage base. The agreement between rocket and tunnel data on the effect of changing tail size is excellent. The flight, rocket, and tunnel data agree well at  $C_L = 0.3$ . In general, the agreement in data from the various sources is good.

#### Douglas D-558-II Airplane

Drag data for  $C_L \approx 0$  and  $0.3$  are presented in figure 3 for models of the Douglas D-558-II research airplane. Data were taken from rocket-model tests by Langley PARD (ref. 5), tests in the Langley 8-foot high-speed and 4-foot supersonic pressure tunnels (refs. 6 and 7), and unpublished flight tests and tests in the Langley 8-foot transonic tunnel. In order to obtain rocket-model data at  $C_L = 0$ , cross plots were made of the data for six different models with tail settings varying from about  $-2^\circ$  to  $-3.7^\circ$ . Data from the Langley 8-foot high-speed and 4-foot



supersonic tunnels were used for tail settings of  $-2^\circ$  at subsonic speeds and  $-4^\circ$  at supersonic speeds; these values were approximately those required for trim at  $C_L = 0$ . Flight data were for tail settings from  $0.3^\circ$  to  $3.3^\circ$  and 8-foot transonic tunnel data were available only for a tail setting of  $0^\circ$ . At  $C_L = 0$ , flight and rocket data were not obtained to sufficiently low speeds to provide a comparison in subsonic drag level but the agreement between rocket and tunnel data in drag-rise Mach number is quite good. Data from the various sources at  $M > 1$  all fall within a band about  $\pm 7$  or 8 percent wide. More detailed comparison is not attempted because of the differences in base size, canopy, wing-tip section thickness, and tail-surface sweep between the various models.

At  $C_L = 0.3$ , the agreement between tunnel and flight data is quite good with the data from the tunnel model (with thinner wing tips, and no canopy at  $M = 1.6$ ) falling slightly lower than the flight data. Unpublished data from later tests in the 4-foot supersonic pressure tunnel show a  $\Delta C_D$  of 0.006 from adding the canopy and extending the vertical tail at  $M = 2.0$ . This increment would improve the agreement between tunnel and flight tests at the higher supersonic speeds.

In general, the agreement in data from the various sources is quite good, considering differences in model geometry.

#### Bell X-5 Airplane

Drag data at  $C_L = 0.2$  are presented in figure 4 for the Bell X-5 research airplane at  $59^\circ$  sweep from flight tests (ref. 8 and later unpublished data) and tests in the Langley 8-foot transonic tunnel (ref. 9). Stabilizer and elevator settings varied from  $-1.4^\circ$  to  $-3.1^\circ$  and from  $+2.50^\circ$  to  $-7.8^\circ$ , respectively, as required during the flight tests. The tunnel drag data were used for the same stabilizer and elevator settings as for the airplane at each Mach number.

The two sets of data show excellent agreement in subsonic level, drag-rise Mach number, and drag level at  $M = 1.03$ . Drag coefficients from the tunnel tests are low compared with flight data in the region between  $M = 0.96$  and 1.0. Discussions with personnel of the Langley 8-Foot and 16-Foot Transonic Tunnel Sections indicate that this difference may result either from model-support interference or from differences between tunnel and flight tests in the interaction between the boundary layer and the wing and body shock waves which, during the transonic drag rise, are moving back to become trailing-edge shock waves. The boundary-layer difference may result from differences in either Reynolds number or surface condition and the relatively thicker boundary layer on the tunnel models would tend to reduce the intensity of the shock waves and drag rise until the shock moves completely off the body at slightly supersonic

speeds. Although the effect noted is not large it is believed worthy of further investigation.

#### McDonnell XF3H-1 Airplane

Minimum drag data are presented in figure 5 for the McDonnell XF3H-1 airplane. Data were taken from flight tests by McDonnell (ref. 10), rocket-model tests by Langley PARD (unpublished data and ref. 11), tests on the Southern California Cooperative Wind Tunnel bump (ref. 12), and tests in the Ordnance Aerophysics Laboratory tunnel at Daingerfield, Texas (ref. 13).

The flight, rocket, and bump data are in very good agreement up to  $M = 1.05$  in subsonic level, drag-rise Mach number, and transonic pressure-drag rise. The marked departure, at  $M = 1.05$ , between rocket and bump data may be due to limitations to the bump test technique for drag tests or to the particular model-bump combination used. Part of the difference at  $M > 1.05$  between rocket and bump data and the difference at  $M = 1.5$  between tunnel data and logical extrapolations of the rocket data appear to be due to the differences between the models. The data in references 11, 22, and 23 show that a model with the XF3H-1 inlet had considerably higher supersonic drag than a faired nose model.

In general, the agreement in the data from the various sources is very good considering the geometric differences between the various models


#### Douglas XF4D-1 Airplane

Minimum drag data are presented in figure 6 for the Douglas XF4D-1 airplane. Data were taken from flight tests by Douglas (unpublished), rocket-model tests by Langley PARD (ref. 14), and tests in the Ames 6- by 6-foot supersonic tunnel (ref. 15).

The agreement in subsonic drag level, drag-rise Mach number, and transonic pressure-drag rise is excellent for the flight, rocket, and tunnel data. The small difference between rocket and tunnel data at supersonic speeds may be due to differences in surface condition and extent of laminar flow between the two models.

#### North American YF-100A Airplane

Minimum drag data for the North American YF-100A airplane are presented in figure 7. Data were taken from rocket-model tests by Langley PARD (unpublished), tests in the Langley 16-foot transonic tunnel



(unpublished), and tests in North American Supersonic Wind Tunnel and Southern California Cooperative Wind Tunnel (refs. 16 and 17).

The agreement of the wind-tunnel and rocket-model drag data is very good throughout the Mach number range covered by the tests. The differences in drag coefficients shown between the tunnel (model B) and rocket-model tests at supersonic speeds may be an effect of Reynolds number or of unknown detail geometric differences between the various models. The reasons for the slightly lower drags shown by the transonic tunnel data (model A) at  $M \approx 1$  are believed to be model-support interference or differences in shock-boundary-layer interaction as discussed for the Bell X-5 data despite the geometric differences noted in figure 7.

#### Republic XF-91 Airplane


Low-lift drag data for the Republic XF-91 airplane are presented in figure 8. Data were taken from Air Force flight tests (ref. 19), Republic flight tests (unpublished), and from Langley PARD rocket-model tests (ref. 18).

The agreement in subsonic drag level, drag-rise Mach number and pressure-drag rise to  $M = 1.0$  is very good. The small differences at subsonic speeds (15 percent maximum) may be due to differences in Reynolds number or surface condition, or to the difference between faired-nose and open-inlet drag. Data in references 22 and 23 indicate that a similar open inlet had less drag than a faired nose; the difference (corrected for ratio of wing area to inlet area) amounts to 0.0036 for  $M < 0.95$ , 0.0030 at  $M = 1$ , and 0 at  $M = 1.15$ .

In general, the rocket-model and airplane drag data are in very good agreement.

#### Reynolds Number Effects

In order to discover any trends or effects on drag of the Reynolds number of the various tests, the drag data presented in figures 1 to 8 were plotted against Reynolds number at constant Mach number. The majority of the data were for the Reynolds number range between  $1 \times 10^6$  and  $10 \times 10^6$  or  $12 \times 10^6$  and thus were in the region where the transition from laminar to turbulent boundary layer would be expected to occur. Since transition is so sensitive to initial air-stream turbulence, fine construction details, and surface roughness, no consistent patterns were discernible in the lower Reynolds number data. For instance, two fairly comparable cases are the Ames 6-foot-tunnel and Langley rocket-model tests of the Douglas X-3 and Douglas XF4D-1 airplanes: for the X-3 the tunnel drag data at  $R \approx 2 \times 10^6$  to  $2.5 \times 10^6$  were lower than rocket data at



$R \approx 6 \times 10^6$  to  $10 \times 10^6$  at subsonic speed and were higher at supersonic speeds which might indicate that the boundary layer had an appreciable length of laminar run and was in a state of transition at subsonic speeds but was almost fully turbulent at supersonic speeds. For the XF<sup>4</sup>D-1 on the other hand the tunnel and rocket data agreed at subsonic speeds but the tunnel values of  $C_D$  were lower at supersonic speeds, which might indicate the existence of a greater extent of laminar flow on the tunnel model at supersonic speeds rather than at subsonic speeds as was indicated for the X-3 tests.


The greatest Reynolds number ranges of the data presented herein are for the Douglas XF<sup>4</sup>D-1 and McDonnell XF<sup>3</sup>H-1 configurations. These data are shown in figure 9 as plots of  $C_D$  against  $R$  at  $M = 0.8$  to  $0.9$ . Also shown in figure 9 are values of skin friction drag  $\left( C_f \frac{\text{Wetted area}}{\text{Wing area}} \right)$  for each configuration where  $C_f$  was obtained for smooth surfaces with turbulent boundary layers at  $M \approx 1$  from reference 24. The level and shape of the "smooth  $C_f$ " curve of reference 24 have been well corroborated by many investigations, reference 25, for example.

The drag data for the XF<sup>3</sup>H-1 and XF<sup>4</sup>D-1 show essentially no effect of Reynolds number in contrast to the marked reduction in  $C_D$  with increased  $R$  shown by the  $C_f$  curve. The analysis of  $C_f$  for rough surfaces presented in reference 24 indicates that an invariance of  $C_D$  with  $R$  might be expected for airplanes with mass-production-type surfaces. The level of  $C_D$  shown in figure 9 is, however, about 0.003 to 0.004 higher than would be estimated from reference 24. It is quite possible, also, that both the airplanes had better than "mass-production" surfaces and the comparatively high  $C_D$  at high  $R$  may result from such items as leakage, gun ports, cooling air, and other items that could not be duplicated properly on the wind-tunnel and rocket models.

In any event, the available data do not indicate that one should depend on obtaining a large reduction in drag for an airplane at high Reynolds numbers over the drag shown by wind-tunnel or rocket-model tests at Reynolds numbers of  $1 \times 10^6$  to  $10 \times 10^6$ .

#### CONCLUDING REMARKS


From the various data comparisons presented in the figures and previously discussed, it appears that good agreement exists in drag data from various sources when care is taken to compare the data under similar conditions of lift, tail setting, inlet mass-flow, and so forth. In cases where appreciable disagreement occurred the prime contributing factor appeared to be geometric differences between the airplane and




various models. No consistent effects of Reynolds number on drag were discernible in the data presented; these effects probably were obscured by such items as differences in details of geometry, surface condition, cooling air flow, and other items for the data from various sources.

Langley Aeronautical Laboratory,  
National Advisory Committee for Aeronautics,  
Langley Field, Va., June 3, 1954.

## REFERENCES

1. Saltzman, Edwin J.: Flight Measurements of Lift and Drag for the Bell X-1 Research Airplane Having a 10-Percent-Thick Wing. NACA RM L53F08, 1953.
  2. Mattson, Axel T., and Loving, Donald L.: Force, Static Longitudinal Stability, and Control Characteristics of a 1/16-Scale Model of the Bell XS-1 Transonic Research Airplane at High Mach Numbers. NACA RM L8A12, 1948.
  3. Peck, Robert F., and Hollinger, James A.: A Rocket-Model Investigation of the Longitudinal Stability, Lift, and Drag Characteristics of the Douglas X-3 Configuration With Horizontal Tail of Aspect Ratio 4.33. NACA RM L53F19a, 1953.
  4. Olson, Robert N., and Chubb, Robert S.: Wind-Tunnel Tests of a 1/12-Scale Model of the X-3 Airplane at Subsonic and Supersonic Speeds. NACA RM A51F12, 1951.
  5. Parks, James H., and Mitchell, Jesse L.: Longitudinal Trim and Drag Characteristics of Rocket-Propelled Models Representing Two Airplane Configurations. NACA RM L9L22, 1950.
  6. Osborne, Robert S.: High-Speed Wind-Tunnel Investigation of the Longitudinal Stability and Control Characteristics of a 1/16-Scale Model of the D-558-2 Research Airplane at High Subsonic Mach Numbers and at a Mach Number of 1.2. NACA RM L9C04, 1949.
  7. Spearman, M. Leroy: Static Longitudinal Stability and Control Characteristics of a 1/16-Scale Model of the Douglas D-558-II Research Airplane at Mach Numbers of 1.61 and 2.01. NACA RM L53I22, 1953.
  8. Bellman, Donald R.: Lift and Drag Characteristics of the Bell X-5 Research Airplane at 59° Sweepback for Mach Numbers from 0.60 to 1.03. NACA RM L53A09c, 1953.
  9. Bielat, Ralph P. and Campbell, George S.: A Transonic Wind-Tunnel Investigation of the Longitudinal Stability and Control Characteristics of a 0.09-Scale Model of the Bell X-5 Research Airplane and Comparison With Flight. NACA RM L53H18, 1953.
  10. Sohn, R. F., Grose, G. G., Allen, D. W., Lacey, T. R., and Gillooly, R. P.: Model XF3H-1 - Analysis of Preliminary Flight Tests Results - Revision 1. Rep. No. 2496, (Contract Noa(s)-10260), McDonnell Aircraft Corp., Aug. 29, 1952.
- 

11. Carter, Howard S., and Merlet, Charles F.: Flight Determination of the Pressure Recovery and Drag Characteristics of a Twin Side-Inlet Model at Transonic Speeds. NACA RM L53E05, 1953.
  12. Pliske, D. R.: Model XF3H-1 - Summary of Transonic Wind Tunnel Tests on a 2% Scale Bump Model - Series I. Rep. 1545, (Contract NOa(s)-10260), McDonnell Aircraft Corp., Mar. 1, 1950.
  13. Krenkel, A. R.: Model XF3H-1 - Supersonic Wind Tunnel Tests at O.A.L. on 1.5% and 4.5% Scale Models. Rep. 1685, (Contract NOa(s)-10260), McDonnell Aircraft Corp., May 19, 1950.
  14. Mitcham, Grady L., and Blanchard, Willard S., Jr.: Low-Lift Drag and Stability Data From Rocket Models of a Modified-Delta-Wing Airplane With and Without External Stores at Mach Numbers From 0.8 to 1.36. NACA RM L53A27, 1953.
  15. Smith, Willard G.: Wind-Tunnel Investigation at Subsonic and Supersonic Speeds of a Model of a Tailless Fighter Airplane Employing a Low-Aspect-Ratio Swept-Back Wing - Effects of External Fuel Tanks and Rocket Packets on the Drag Characteristics. NACA RM A52J31, 1953.
  16. Mardin, H. R.: Supersonic Wind Tunnel Tests of the 0.02 Scale Full Span Model of the NA-180 (YF-100A) Airplane Through a Mach Number Range of 0.70 to 2.87 To Determine the Effect of Modifications to the Basic Model Components on the Aerodynamic Characteristics. Rep. No. SAL-43, North American Aviation, Inc., Oct. 30, 1952.
  17. Safier, Irving: Report on Wind Tunnel Tests of a 0.07-Scale Sting-Mounted Model of the North American (Inglewood) F-100A (NA-180) Airplane at High Subsonic Speeds and  $M = 1.20$ . CWT Rep. 258, Southern Calif. Cooperative Wind Tunnel, Sept. 4, 1952.
  18. Mitcham, Grady L., and Blanchard, Willard S., Jr.: Summary of the Aerodynamic Characteristics and Flying Qualities Obtained From Flights of Rocket-Propelled Models of an Airplane Configuration Incorporating a Sweptback Inversely Tapered Wing at Transonic and Low-Supersonic Speeds. NACA RM L50G18a, 1950.
  19. Coleman, Robert V., and Cochran, John T.: Phase II Flight Tests of the XF-91 Airplane MR No. MCRFT-2272, USAF No. 46-680 Air Materiel Command, U. S. Air Force, April 1, 1950.
  20. Whitcomb, Richard T.: A Study of the Zero-Lift Drag-Rise Characteristics of Wing-Body Combinations Near the Speed of Sound. NACA RM L52H08, 1952.
- 


21. Hall, James Rudyard: Comparison of Free-Flight Measurements of the Zero-Lift Drag Rise of Six Airplane Configurations and Their Equivalent Bodies of Revolution at Transonic Speeds. NACA RM L53J21a, 1954.
  22. Sears, Richard I., and Merlet, C. F.: Flight Determination of the Drag and Pressure Recovery of an NACA 1-40-250 Nose Inlet at Mach Numbers From 0.9 to 1.8. NACA RM L50L18, 1951.
  23. Sears, Richard I.: Some Considerations Concerning Inlets and Ducted Bodies at Mach Numbers From 0.8 to 2.0. NACA RM L53I25b, 1953.
  24. Gollos, W. W.: Boundary Layer Drag for Non-Smooth Surfaces. U. S. Air Force Project RAND RM-1129, The RAND Corp., June 24, 1953.
  25. Mottard, Elmo J., and Lopper, J. Dan.: Average Skin-Friction Drag Coefficients from Tank Tests of a Parabolic Body of Revolution (NACA RM-10). NACA TN 2854, 1953. Rep. 1161, 1954.
- 

TABLE I.- GEOMETRIC CHARACTERISTICS OF THE VARIOUS AIRPLANE CONFIGURATIONS

Characteristics	Configuration					
	Bell X-1	Douglas X-3	Douglas D-558-II	Bell X-5	McDonnell XF3H-1	Douglas XF4D-1
Wing:						
Area, sq ft	130.0	166.5	175.0	a184.3, b186.3	445.0	557.0
Total	130.0	166.5	175.0	a184.3, b186.3	445.0	557.0
Exposed	103.5	108.2	135.0	a184.3, b186.3	357.0	550.0
Mean aerodynamic chord, ft	4.81	7.84	7.5	a10.05, b10.35	12.2	18.25
Aspect ratio	6.0	3.09	3.57	a2.16, b1.94	3.0	2.01
Taper ratio	0.50	0.39	0.57	a0.41, b0.42	0.5	0.33
Sweep	0° at 0.40c	15.9° at c/4	35° at 0.30c	59° at c/4	45° at c/4	52.5° at L.E.
Airfoil						
Root	NACA 65-110 (a = 1) mod.	Faired hexagon	NACA 65-010	NACA 64(10)A011	NACA 0009-1.16	NACA 0007-63/50 - 9.5° mod.
Tip	NACA 65-110 (a = 1) mod.	Faired hexagon	a,cNACA 65-012, bNACA 65-010	NACA 64(08)A008.28	NACA 0007-1.16	NACA 0004.5-63/50 - 6.6° mod.
Laid out 1 to	0.10	0.045	0.098	0.38c	Span	Span
Root-mean square t/c (streamwise)	0.077	0.057	0.082	0.057	0.082	0.06
Horizontal tail:						
Area, sq ft	26.0	f30.9, g43.2	40.8	a51.5, b55.0	69.7	71.74
Total	24.5	f26.6, g39.1	36.0	a27.0, b27.0	57.4	68.5
Exposed	5.0	f3.0, g4.38	3.58	a2.9, b2.94	3.0	4.0
Aspect ratio	0.5	f0.40, g0.40	0.50	45° at c/4	0.50	1.0
Taper ratio	12° at L.E.	f29.3° at c/4	c46° at 0.30c		45° at c/4	45° at c/4
Sweep		810.3° at c/4	a,b40° at 0.30c			
Airfoil						
Root	NACA 65-008	Faired hexagon	NACA 65-010 mod.	NACA 65A006	NACA 0007-1.16	Republic R-4, 40-010
Tip	NACA 65-008	Faired hexagon	NACA 65-010 mod.	NACA 65A006	NACA 0007-1.16	Republic R-4, 40-010
Laid out 1 to	Span	Span	0.30c	Span	Span	Span
Root-mean-square t/c (streamwise)	0.08	0.05	0.069, a,b0.077	0.06	0.07	0.077
Vertical tail (dorsal fins not included):						
Area, sq ft	34.8	23.7	c,d46.5, a,e60.2	a29.5, b31.7	48.2	72.5
Total	27.4	20.3	c,d41.0, a,e44.7	a25.5, b27.7	1.12	46.8
Exposed	1.96	1.31	e,d0.87, a,e1.07	a1.32, b1.51	0.50	2.08
Aspect ratio	0.35	0.29	e,d0.30, a,e0.20	45° at L.E.	45° at c/4	0.26
Taper ratio	0° at 0.40c	38.4° at c/4	45° at 0.30c			66.6° at L.E.
Sweep						
Airfoil						
Root	NACA 65-008	Faired hexagon	NACA 65-010 mod.	NACA 65A006	NACA 0007-1.16	NACA 0008-63/50 - 9°
Tip	NACA 65-008	Faired hexagon	NACA 65-010 mod.	NACA 65A006	NACA 0007-1.16	NACA 0008-63/50 - 6° 45'
Laid out 1 to	Span	Span	0.30c	Span	Span	Span
Root-mean-square t/c (streamwise)	0.08	0.045	0.073	0.06	0.07	0.07

<sup>a</sup>Airplane.  
<sup>b</sup>Wind-tunnel model.  
<sup>c</sup>Rocket model.  
<sup>d</sup>Wind-tunnel model A.

<sup>e</sup>Wind-tunnel model B.  
<sup>f</sup>Tail 1.  
<sup>g</sup>Tail 2.

TABLE I.- GEOMETRIC CHARACTERISTICS OF THE VARIOUS AIRPLANE CONFIGURATIONS - Concluded

Characteristics	Configuration						
	Bell X-1	Douglas X-3	Douglas D-558-II	Bell X-5	McDonnell XF3H-1	Douglas XF4D-1	North American YF-100A
Fuselage:							
Length, ft	31.0	62.75	42.0	a <sub>31.7</sub> , b <sub>32.1</sub>	59.4	40.5	c <sub>46.6</sub> , a <sub>43.3</sub>
Total . . . . .	-----	49.5	-----	b <sub>20.3</sub>	45.8	-----	-----
To exit . . . . .	-----	-----	-----	-----	-----	-----	-----
Maximum frontal area	17.5	27.8	19.6	26.2	26.5	25.0	26.4
(ducts included), sq ft . . . . .	0.135	0.167	0.111	a <sub>0.143</sub> , b <sub>0.141</sub>	0.064	0.045	0.070
Max. frontal area . . . . .	-----	-----	-----	-----	-----	-----	-----
Total wing area	4.72	5.95	5.0	5.79	5.81	5.64	5.80
Maximum equivalent	-----	-----	-----	-----	-----	-----	-----
diameter, ft . . . . .	6.6	10.5	8.4	a <sub>5.45</sub> , b <sub>5.55</sub>	9.8	7.18	c <sub>6.95</sub> , a <sub>6.45</sub>
Total . . . . .	-----	8.3	-----	b <sub>3.51</sub>	7.9	-----	-----
To exit . . . . .	-----	-----	-----	-----	-----	-----	-----
Approximate volume (ducts	320	1262	490	a <sub>388</sub> , b <sub>397</sub>	941	640	c <sub>590</sub> , a <sub>585</sub>
included), cu ft . . . . .	-----	-----	-----	-----	-----	-----	-----
Approximate wetted area	325	744	460	a <sub>352</sub> , b <sub>365</sub>	739	635	c <sub>740</sub> , a <sub>730</sub>
(base and inlet area	0	4.16	0	b <sub>1.72</sub>	3.72	4.28	b <sub>0</sub> , a <sub>4.9</sub>
not included), sq ft . . . . .	-----	-----	-----	-----	-----	-----	-----
Inlet area, sq ft . . . . .	1.26	a <sub>7.9</sub> , b <sub>9.7</sub>	a <sub>5.2</sub> , b <sub>5.41</sub>	b <sub>1.72</sub> (exit)	7.68	5.5	c <sub>6.45</sub> , a <sub>6.80</sub>
Total base area (ducts	-----	-----	-----	b <sub>2.17</sub> (string)	-----	-----	-----
included), sq ft . . . . .	-----	-----	-----	-----	-----	-----	-----
Complete configuration:							
Approximate total wetted area	690	f <sub>1077</sub> , g <sub>1089</sub>	a <sub>5900</sub> , b <sub>510</sub>	a <sub>744</sub> , b <sub>764</sub>	1622	1335	c <sub>1539</sub> , a <sub>1553</sub>
(ducts included), sq ft . . . . .	5.0	f <sub>6.49</sub> , g <sub>6.52</sub>	a <sub>5.1</sub> , b <sub>5.2</sub>	a <sub>4.04</sub> , b <sub>4.09</sub>	3.91	2.40	c <sub>4.09</sub> , a <sub>4.13</sub>
Total wetted area . . . . .	-----	0.8	-----	0.88	1.0(see text)	0.6	-----
Total wing area	-----	-----	-----	-----	-----	-----	-----
Duct mass flow ratio	-----	-----	-----	-----	-----	-----	-----
at M = 1 . . . . .	-----	-----	-----	-----	-----	-----	0.9*
Equivalent body:							
Frontal area, sq ft . . . . .	-----	31.0	28.9	24.1	-----	46.6	-----
Maximum diameter, ft . . . . .	-----	6.28	6.06	5.52	-----	7.7	-----
L/D <sub>max</sub>	-----	-----	-----	-----	-----	-----	-----
Total . . . . .	-----	10.0	7.66	6.12	-----	5.9	-----
To exit . . . . .	-----	7.8	6.94	3.65	-----	5.26	-----
Volume, cu ft . . . . .	-----	1163	695	a <sub>412</sub> , b <sub>420</sub>	-----	920	-----
Source:							
Flight tests	1	-----	Unpublished	8	10	Unpublished	19 and unpublished
Reference . . . . .	-----	-----	-----	-----	-----	-----	-----
Rocket-model tests	-----	3	5	-----	Unpublished and 11	14	Unpublished
Reference . . . . .	-----	-----	-----	-----	-----	-----	-----
Model scale . . . . .	0.0625	0.16	0.129	-----	0.10 and 0.147	0.10	0.11
Wind-tunnel tests	2 and unpublished	4	6 and 7	9	12 and 13	15	16, 17, and unpublished
Reference . . . . .	0.0625	0.083	0.0625	0.09	0.02 and 0.015	0.055	0.02, 0.07, and 0.15
Model scale . . . . .	and 0.250	-----	-----	-----	-----	-----	-----

\*Airplane.

bWind-tunnel model.

cRocket model.

dWind-tunnel model A.

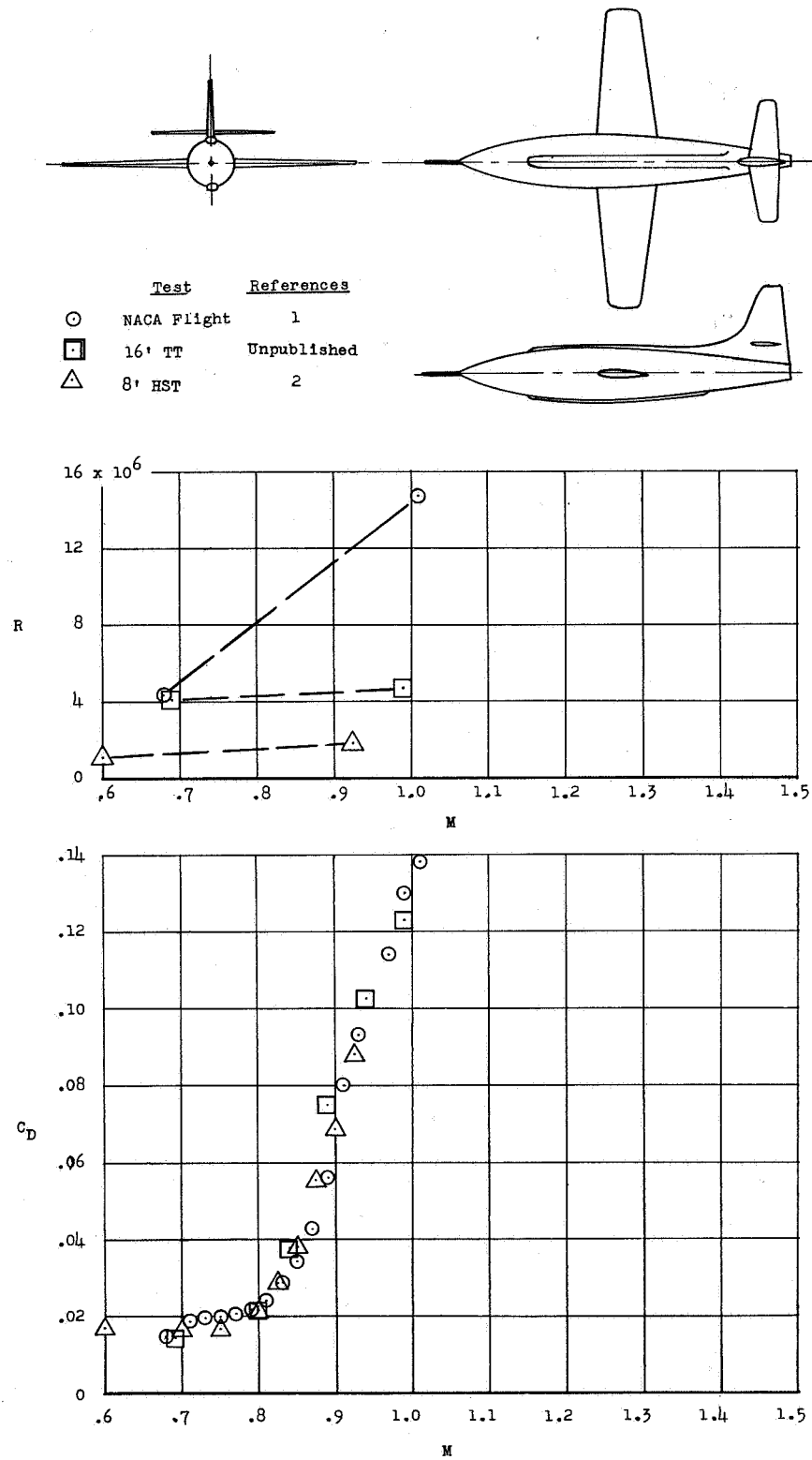


Figure 1.- Bell X-1 airplane (10-percent wing).  $C_L = 0.2$ .

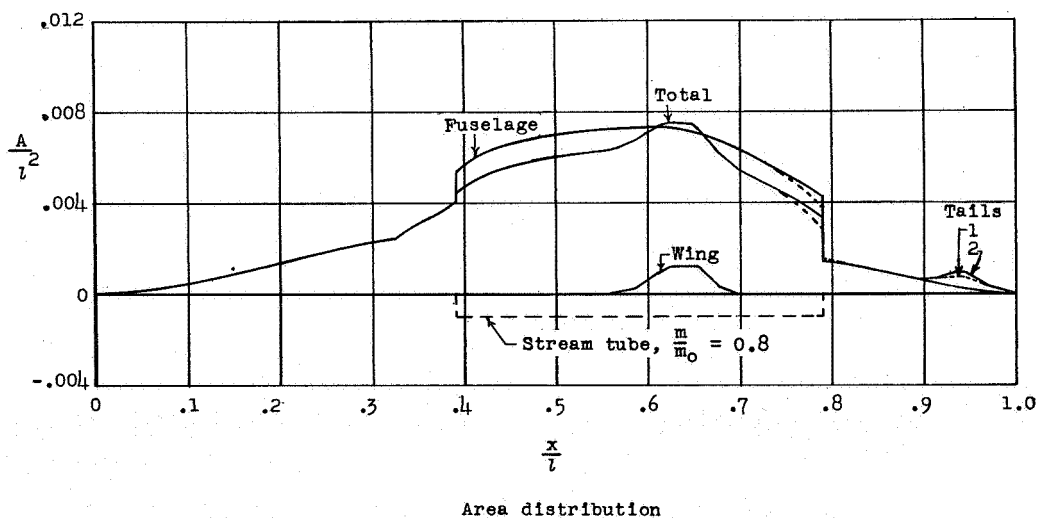
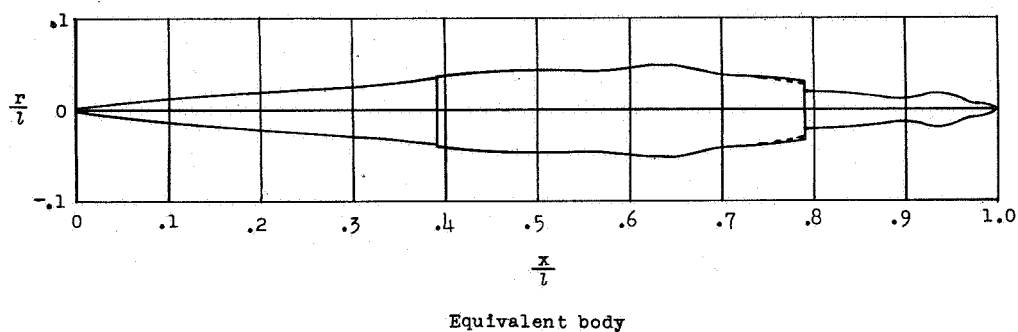
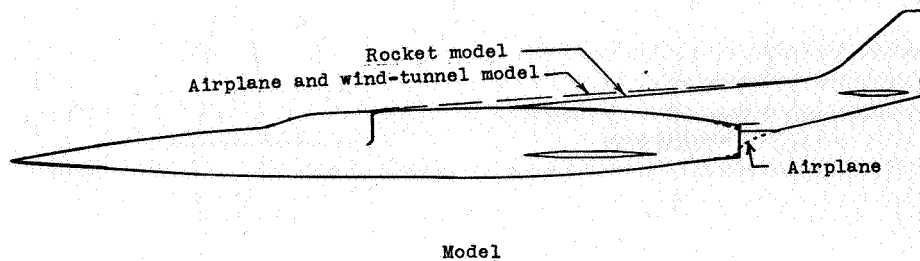


Figure 2.- Douglas X-3 airplane.  $C_L \approx 0$  and 0.3.

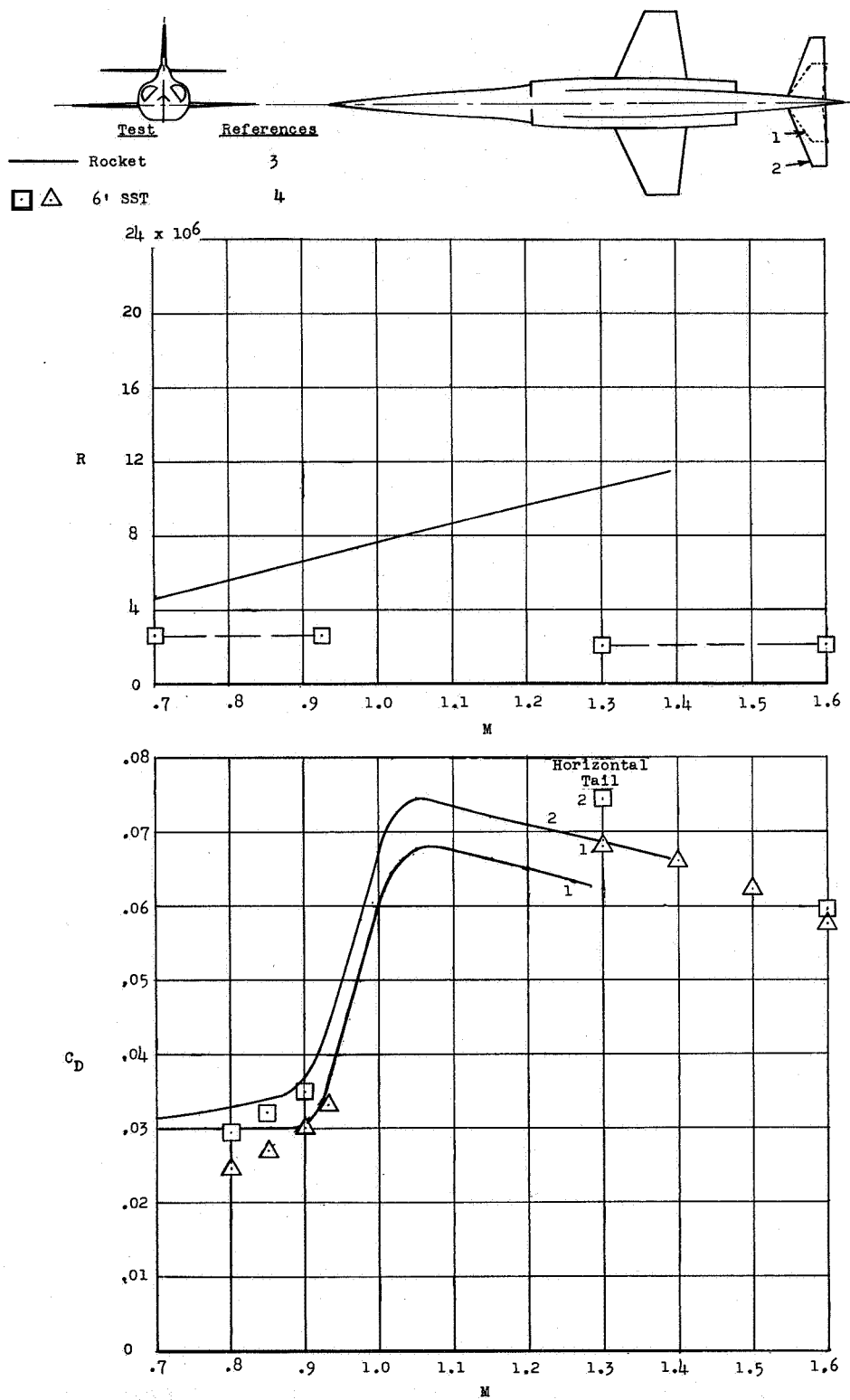


Figure 2.- Continued.  $C_L \approx 0$ .

Test	References
○ DAC-NACA Flight	Unpublished ( $13 \times 10^6 < R < 37 \times 10^6$ )
— Rocket	3
□ 6'SST	4

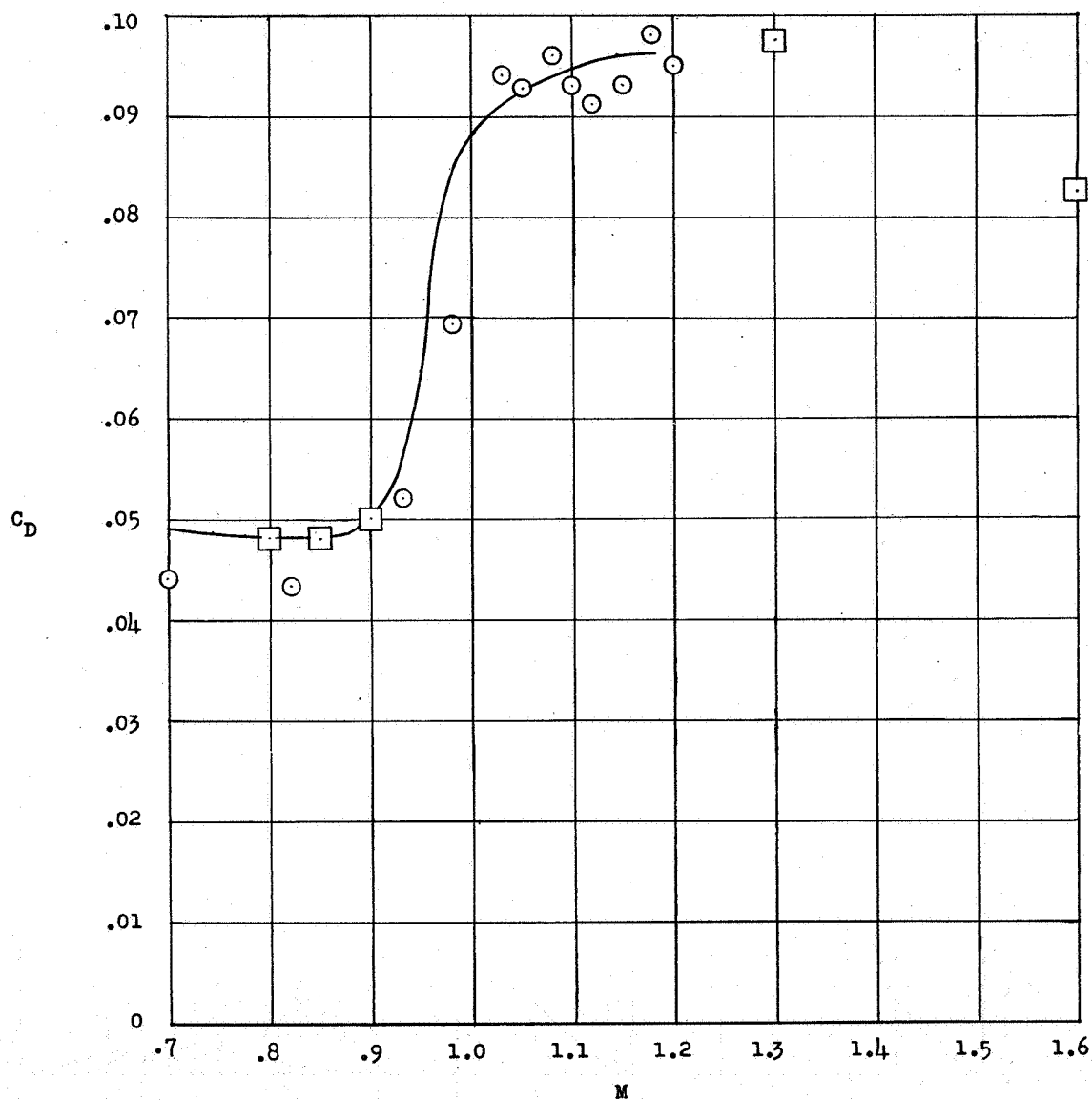


Figure 2.- Concluded.  $C_L = 0.3$  (Tail 2).

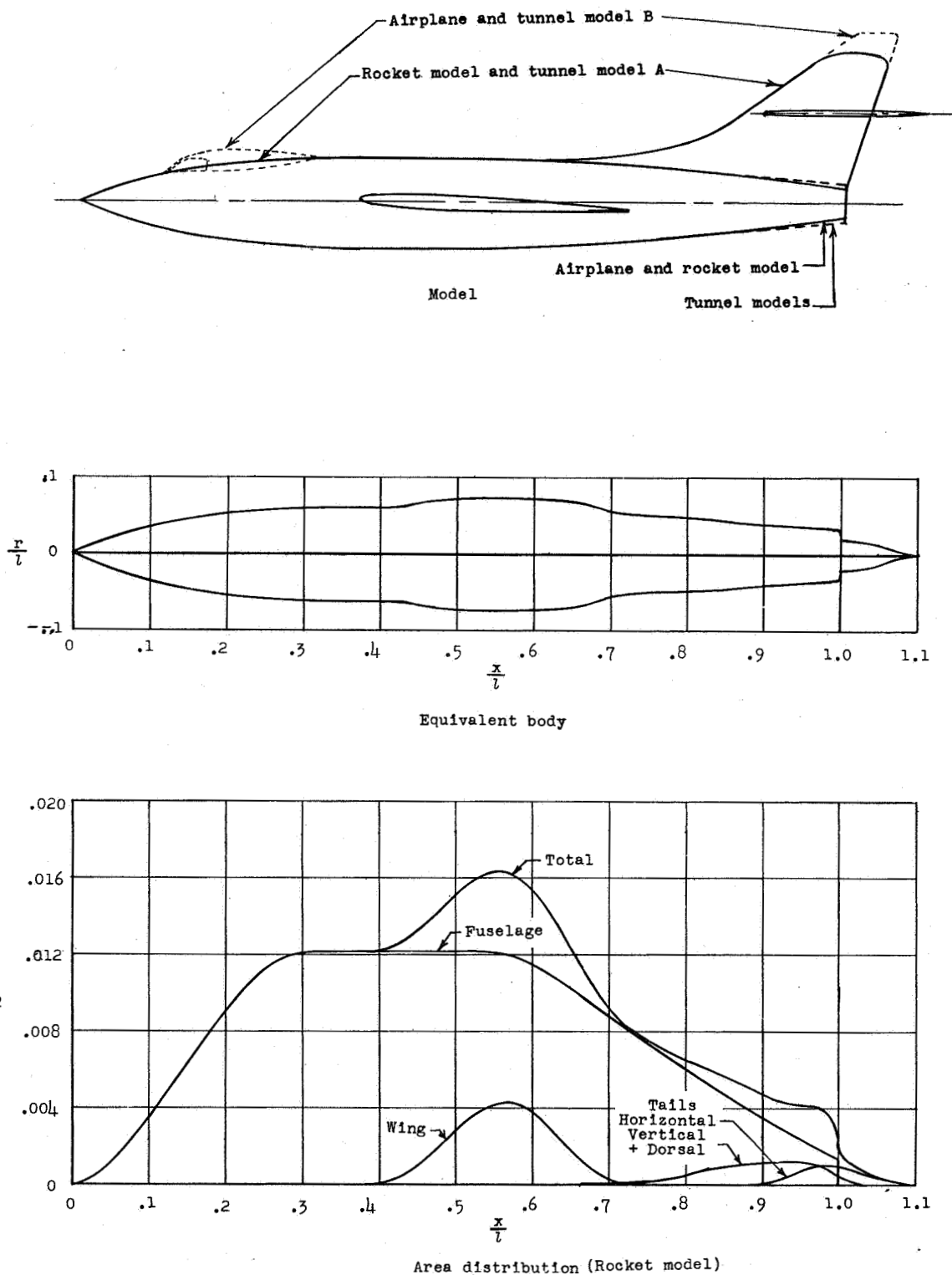
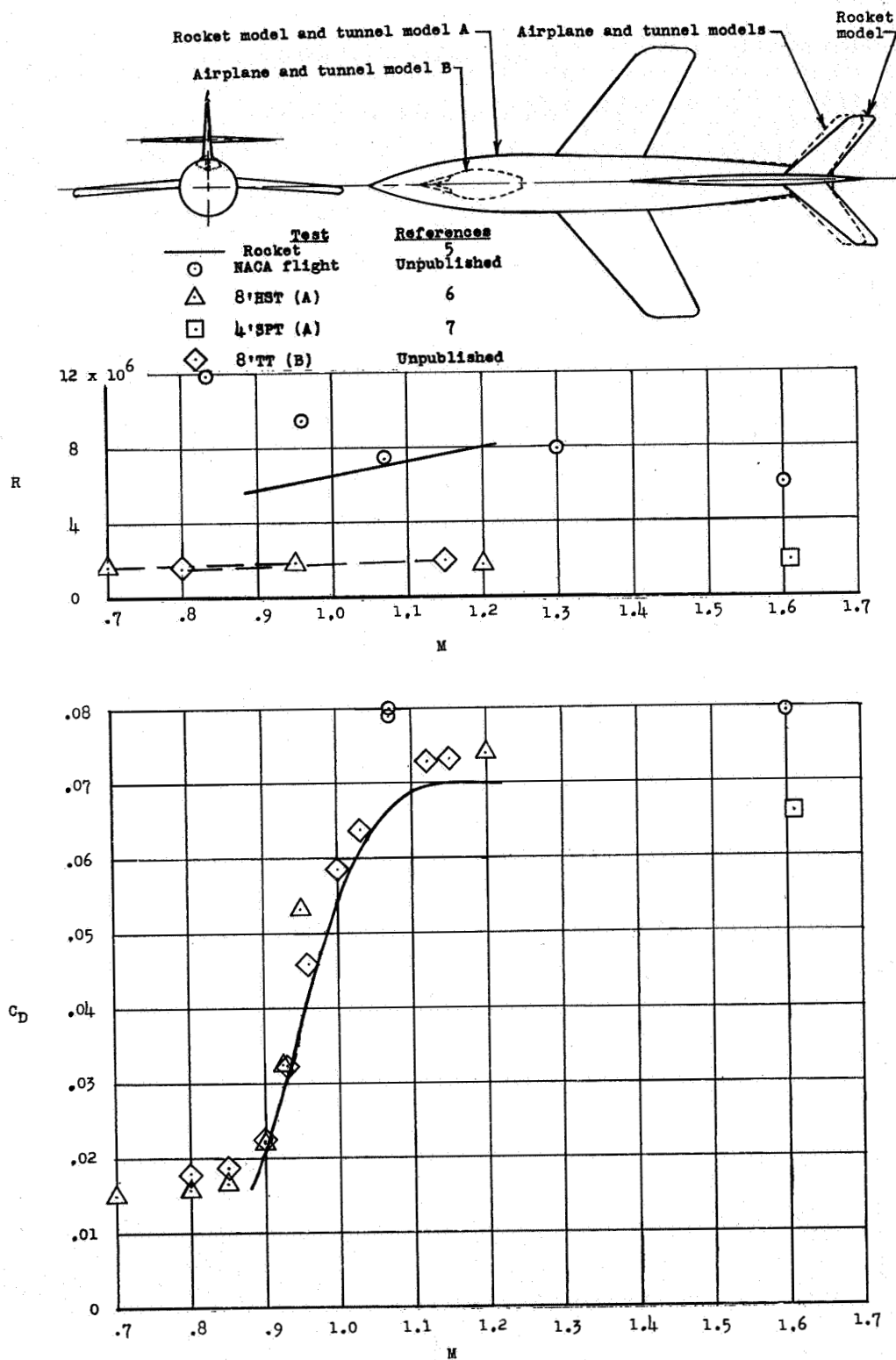
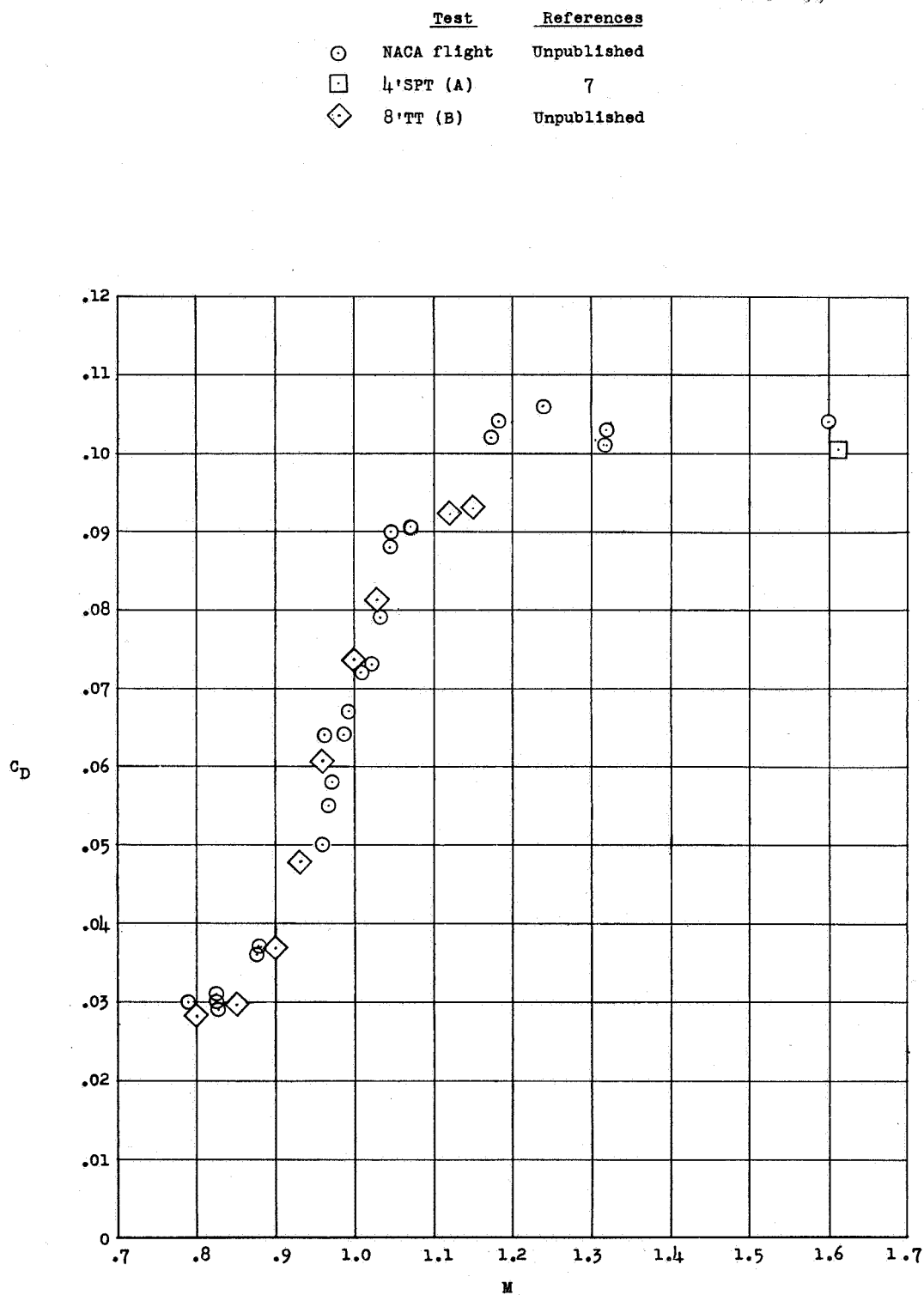


Figure 3.- Douglas D-558-II airplane.  $C_L \approx 0$  and 0.3.



Figure 3.- Concluded.  $C_L \approx 0.3$ .

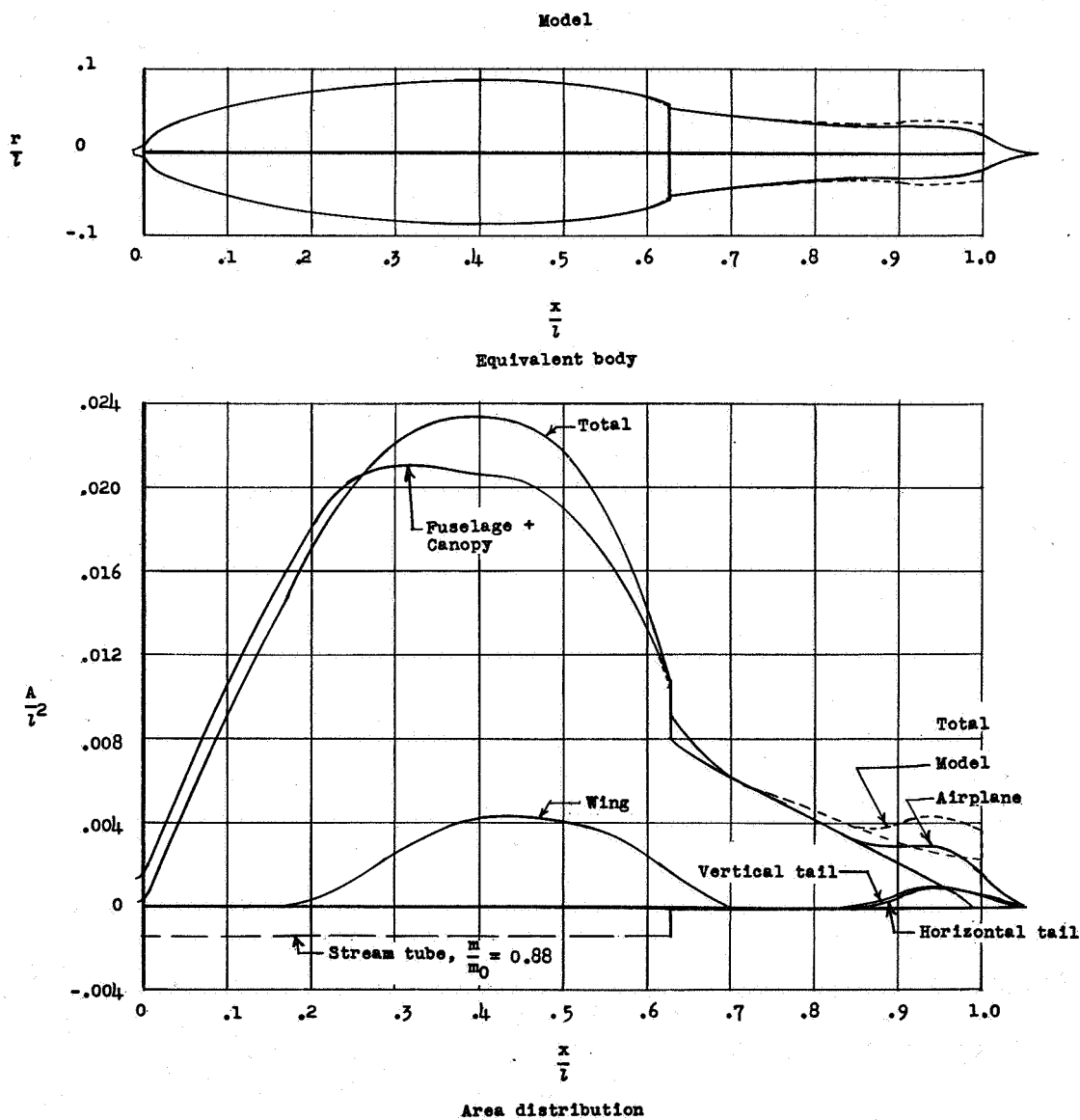
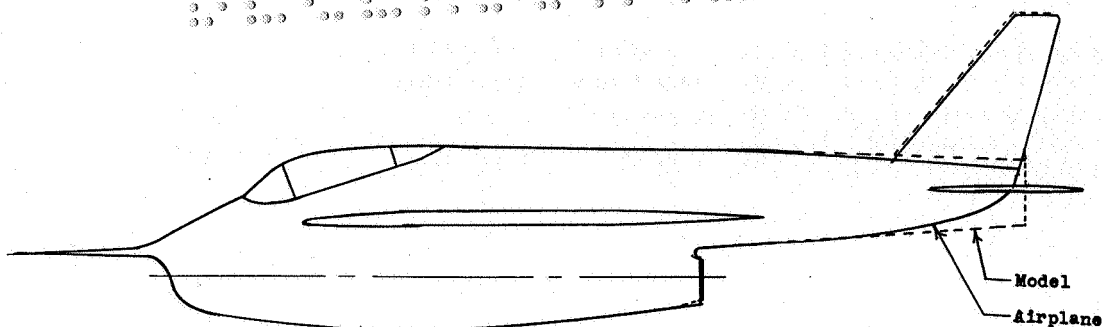
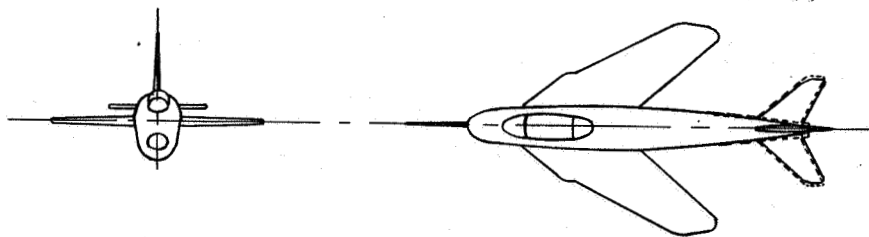


Figure 4.- Bell X-5 airplane (59° sweep).  $C_L = 0.2$ .



Test	References
○ NACA Flight	8
○ NACA Flight	Unpublished
△ 8'TT	9

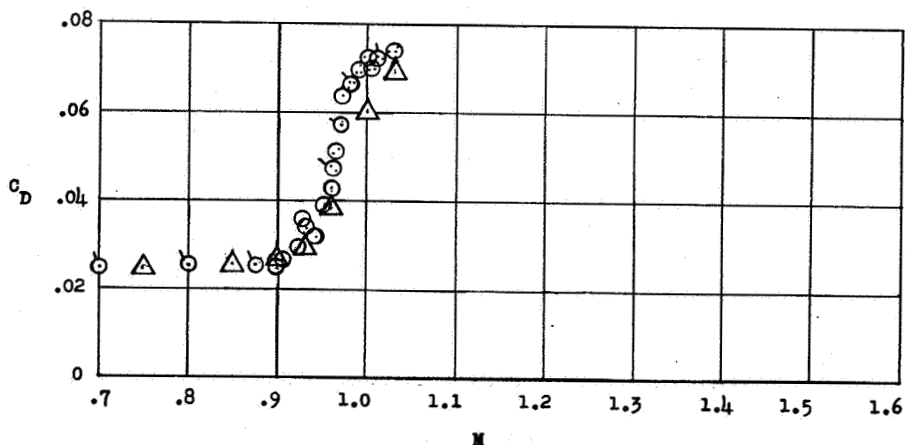
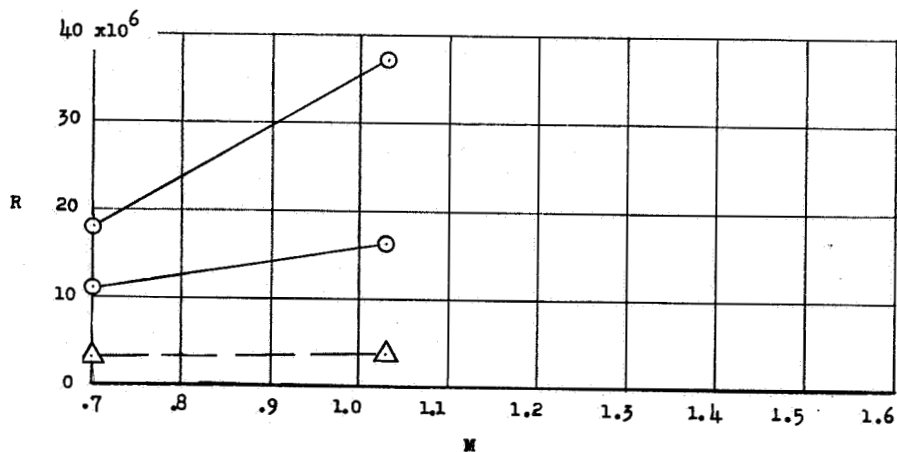
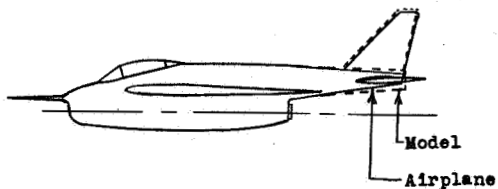
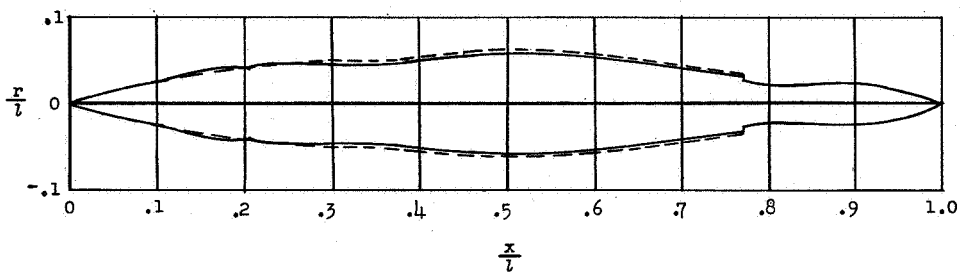
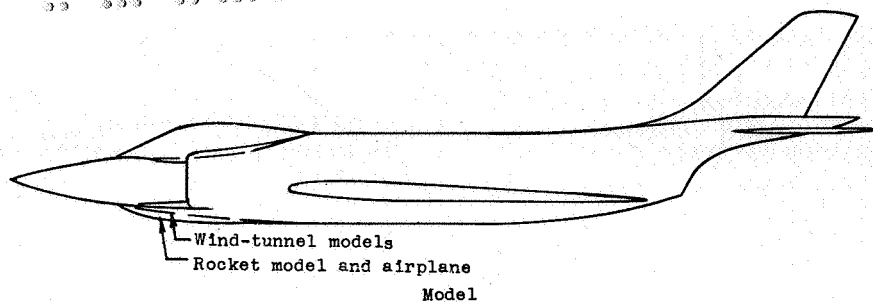
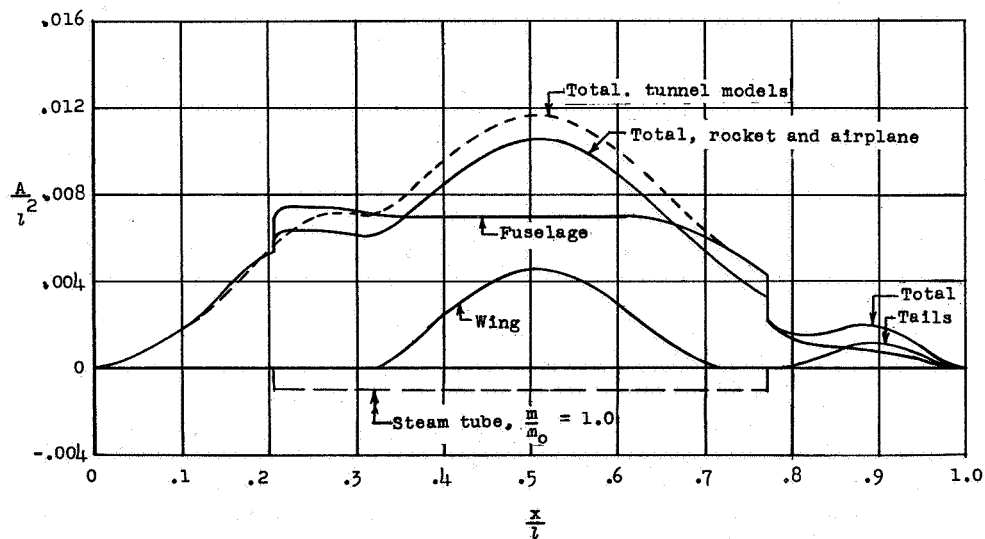


Figure 4.- Concluded.



Equivalent body



Area distribution

Figure 5.- McDonnell XF3H-1 airplane.  $C_L \approx 0$ .

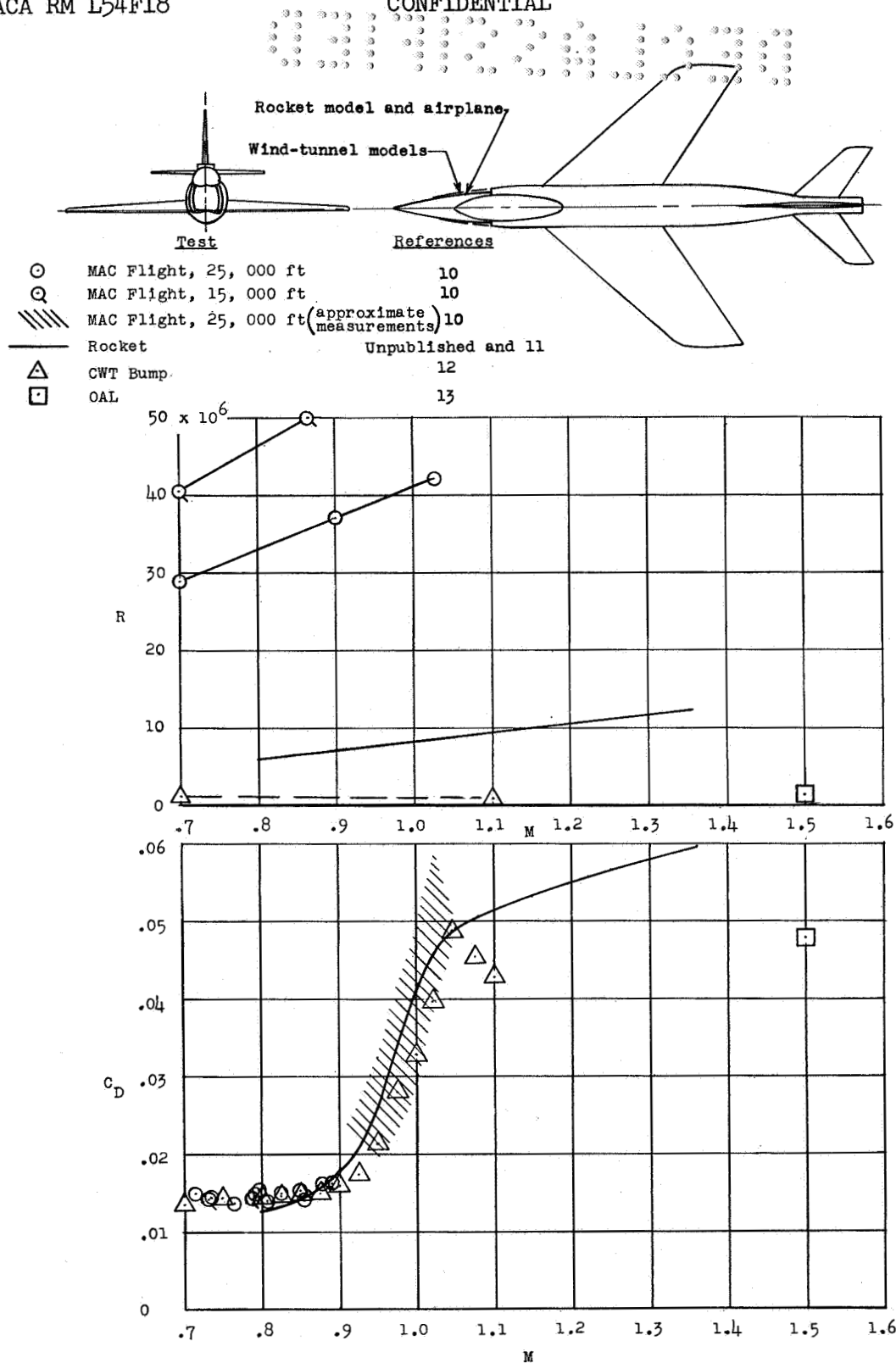


Figure 5.- Concluded.

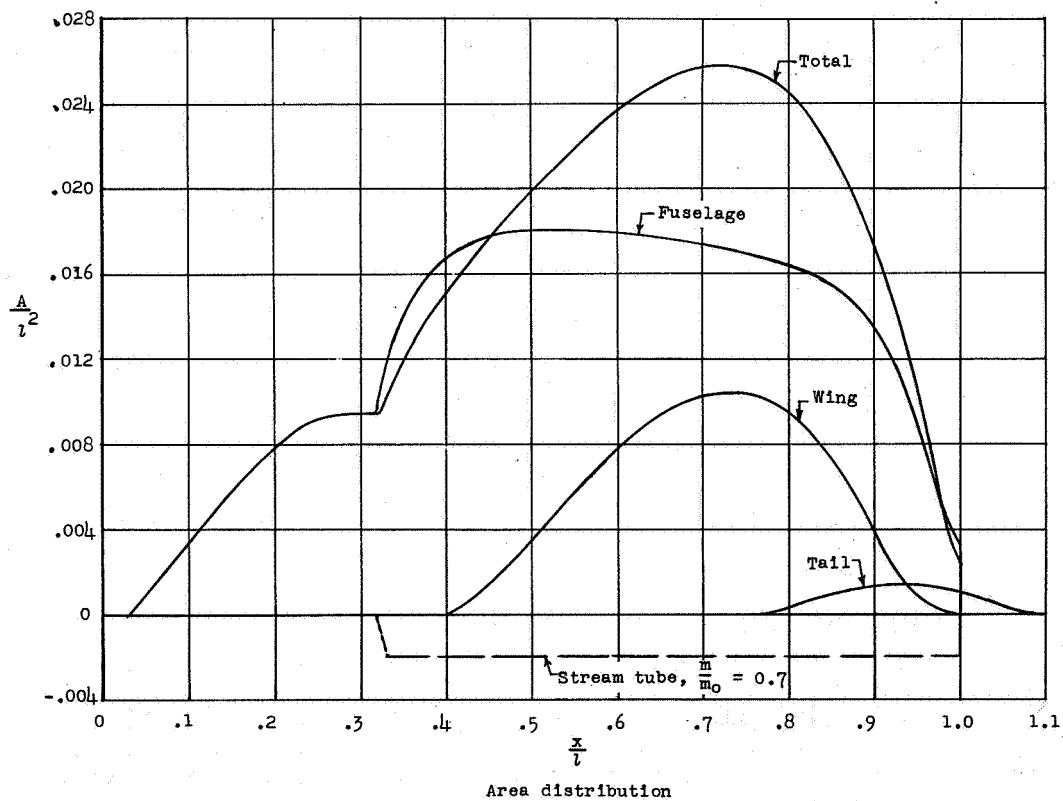
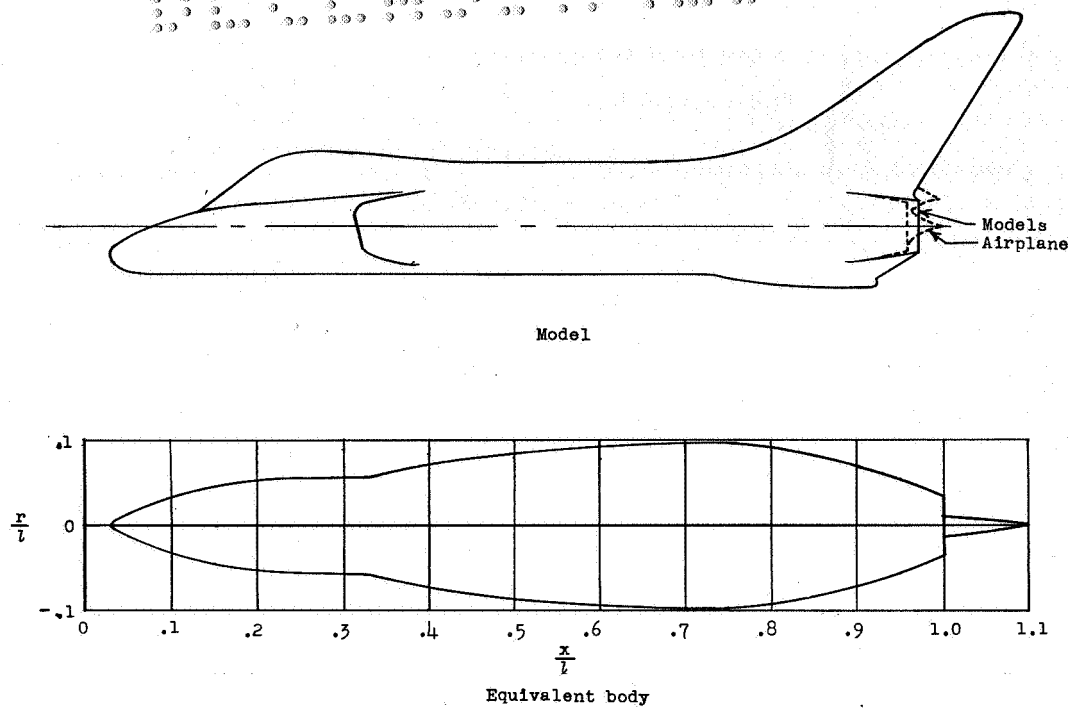


Figure 6.- Douglas XF4D-1 airplane.  $C_L \approx 0$ .

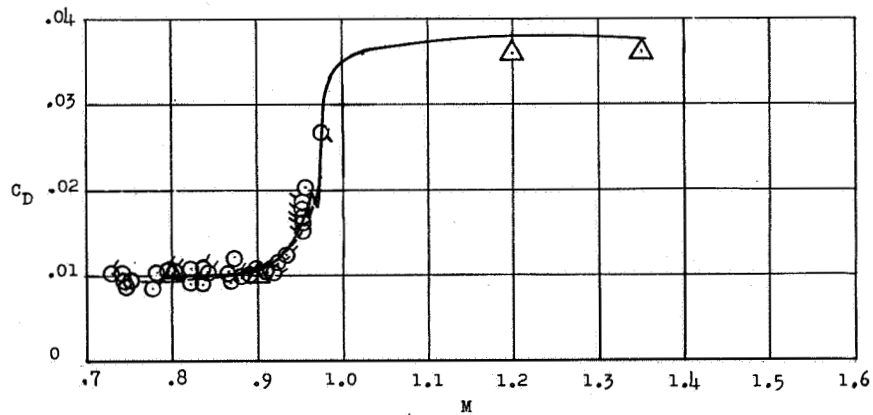
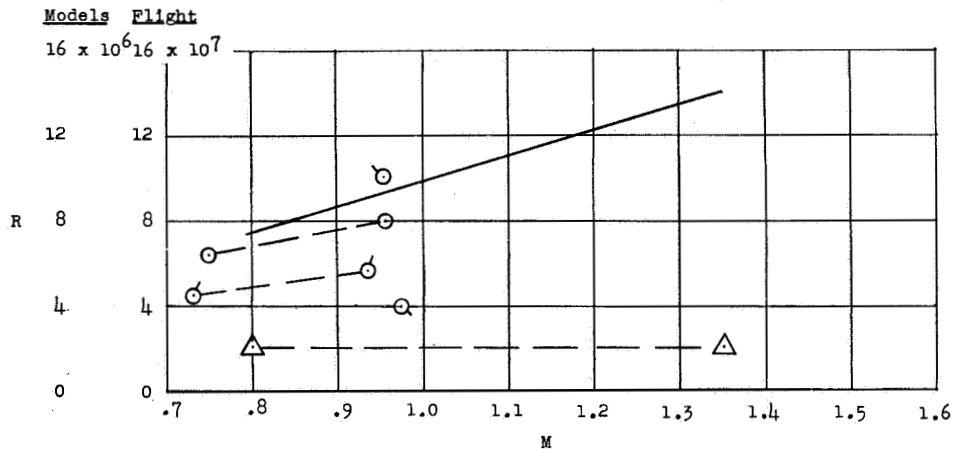
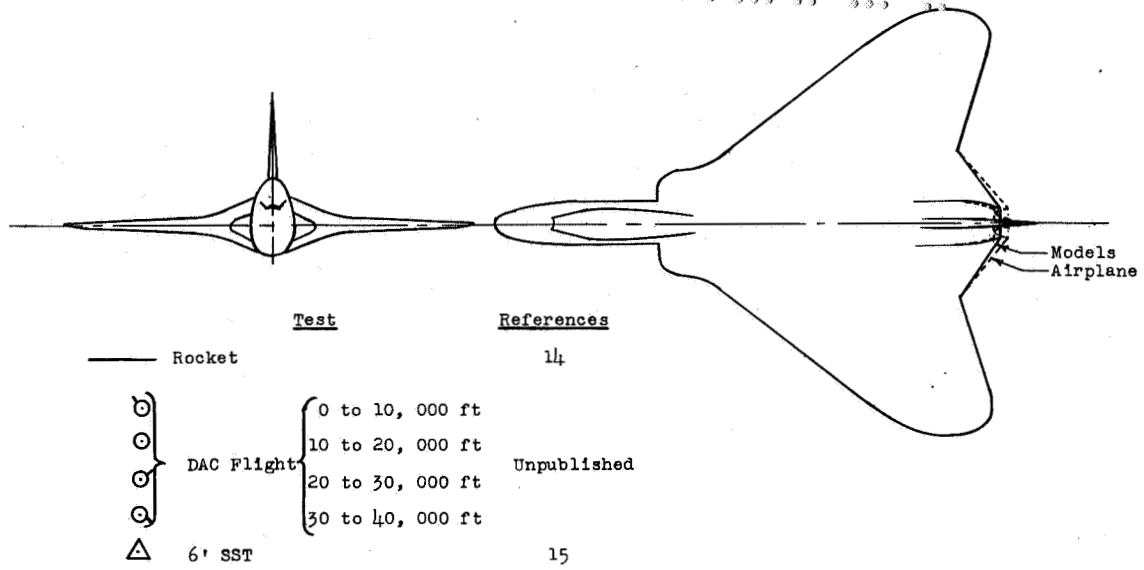
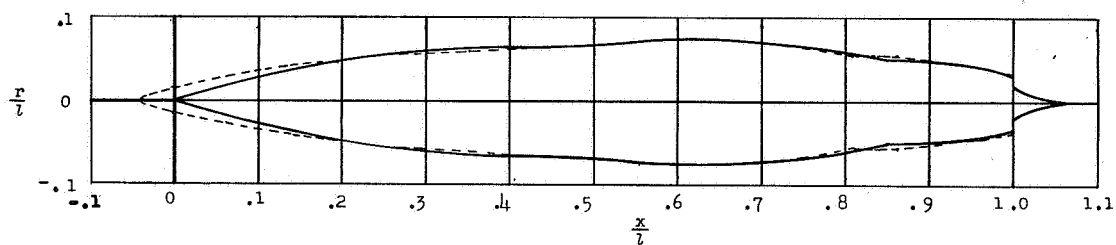
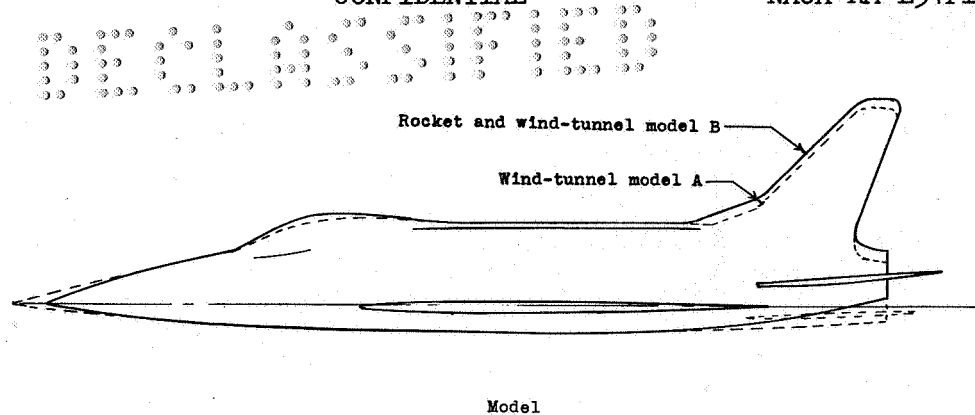
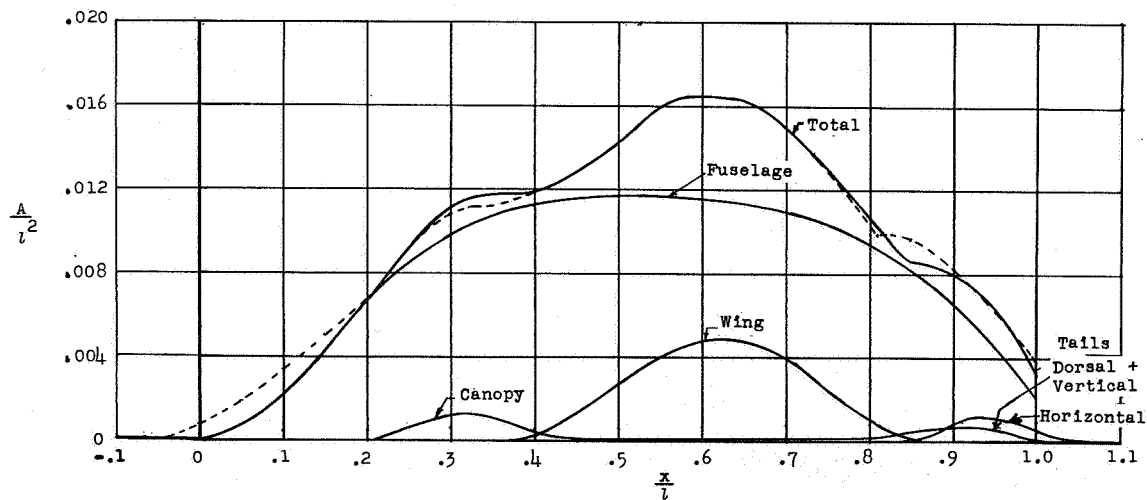


Figure 6.- Concluded.



Equivalent body



Area distribution

Figure 7.- North American YF-100A airplane.  $C_L \approx 0$ .

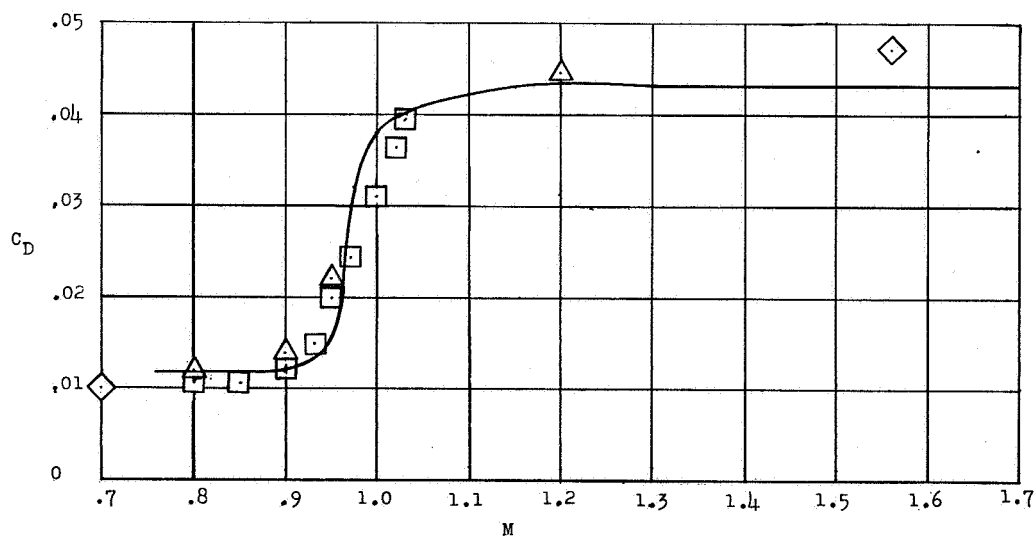
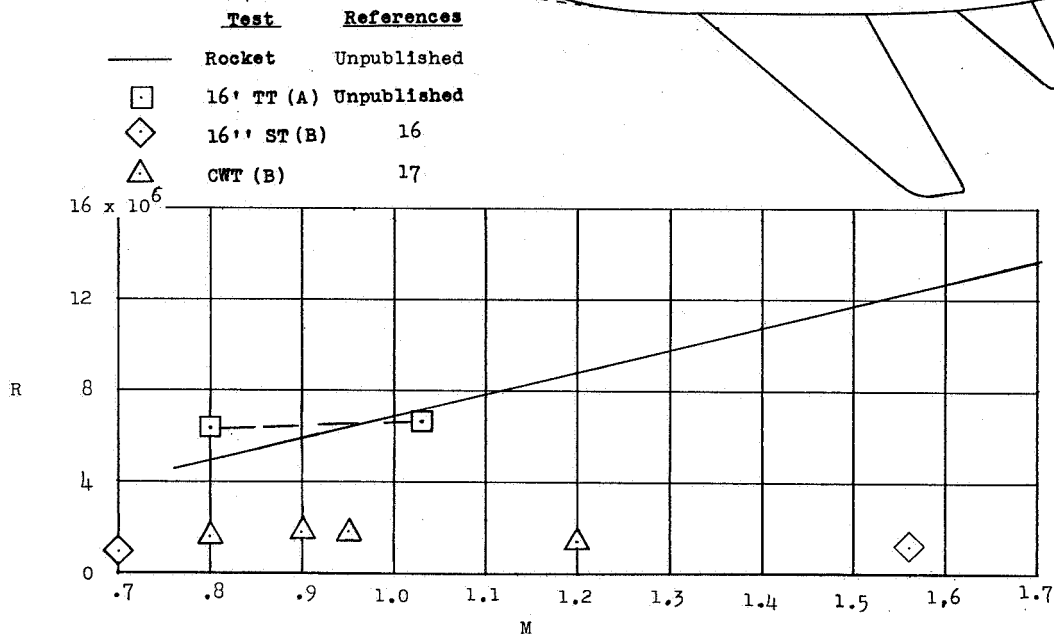
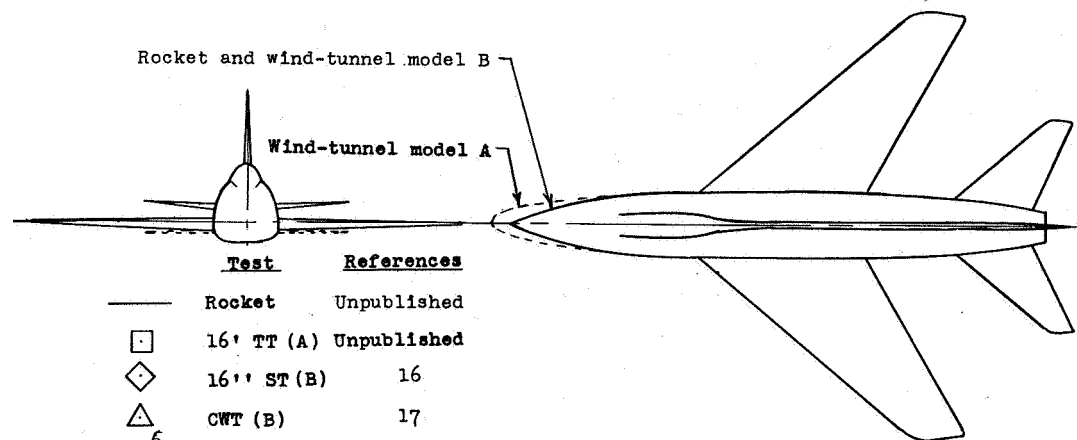
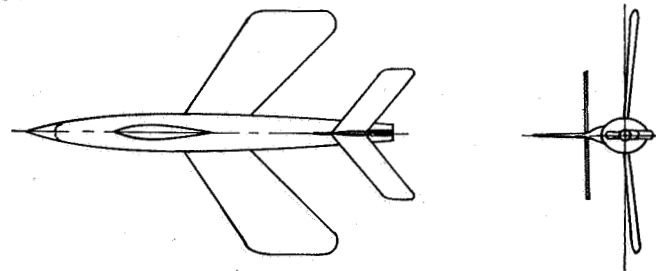
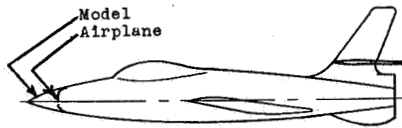


Figure 7.- Concluded.



Model  
Airplane



Test

Rocket,  $C_L = 0$

{ USAF and RAC Flight,  $C_L \approx 0$   
zero rocket thrust

References

18

19 and  
Unpublished

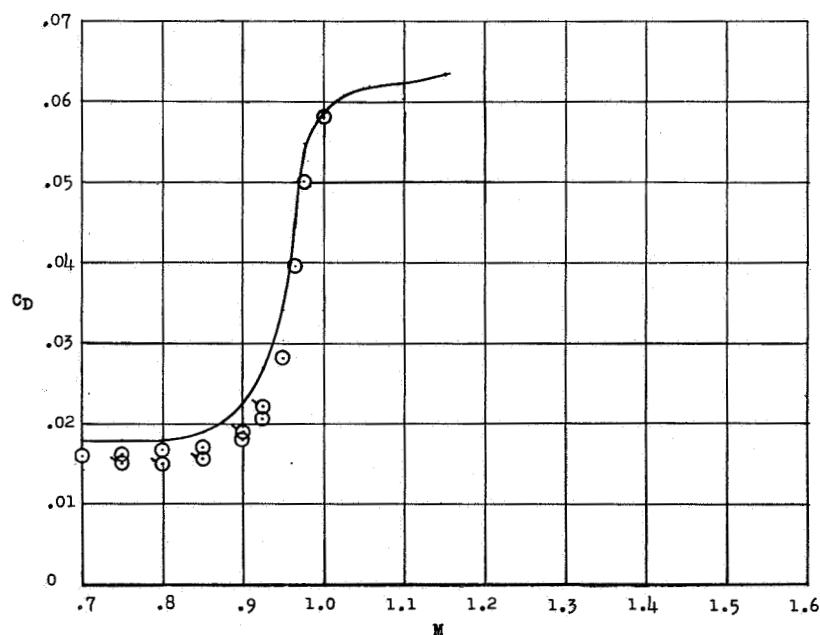
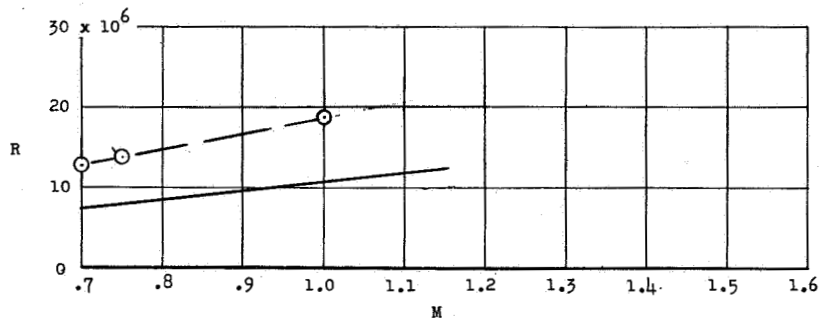
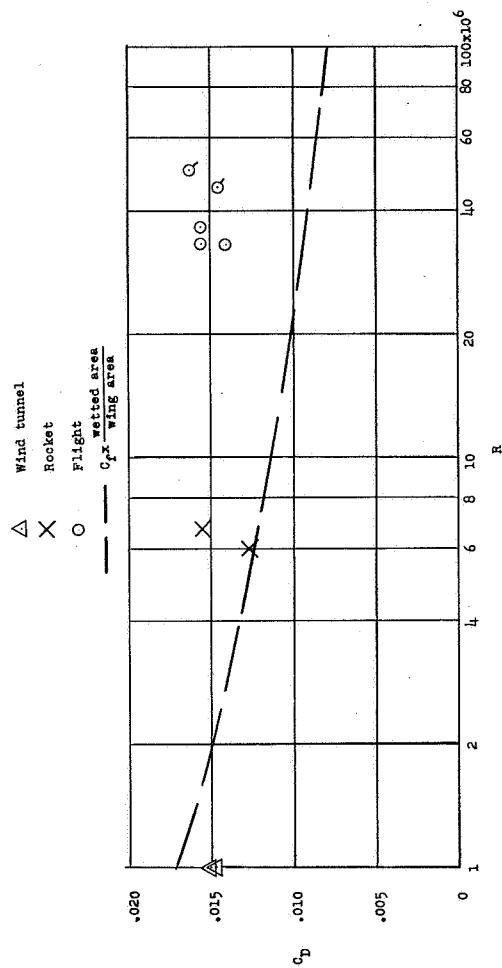
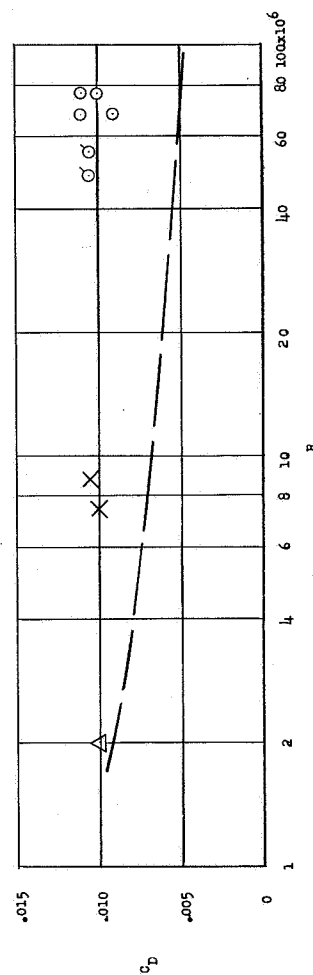


Figure 8.- Republic XF-91 airplane.  $C_L \approx 0$ .



(a) McDonnell XF3H-1 airplane. Data from figure 5.



(b) Douglas XF4D-1 airplane. Data from figure 6.

Figure 9.- Comparison of  $C_D$  from tests at various Reynolds numbers.  
M = 0.8 to 0.9.

